Department of Electrical Engineering

Resistive Loss Modelling for Inverter-fed Induction Motors

Huynh Van Khang

Aalto University

DOCTORAL DISSERTATIONS

Aalto University publication series
DOCTORAL DISSERTATIONS 162/2012

Resistive Loss Modelling for Inverter-fed Induction Motors

Huynh Van Khang

A doctoral dissertation completed for the degree of Doctor of Science in Technology to be defended, with the permission of the Aalto University School of Electrical Engineering, at a public examination held at the lecture hall S1 of the school on 21 December 2012 at 12.

Aalto University
School of Electrical Engineering
Department of Electrical Engineering
Electromechanics

Supervising professor
Prof. Antero Arkkio

Preliminary examiners
Prof. Andrea Cavagnino, Politecnico di Torino, Italy.

Prof. Gorazd Štumberger, University of Maribor, Slovenia.

Opponent
Prof. Chang-Seop Koh, Chungbuk National University, Korea

Aalto University publication series
DOCTORAL DISSERTATIONS 162/2012

ISBN 978-952-60-4891-8 (printed)
ISBN 978-952-60-4892-5 (pdf)
ISSN-L 1799-4934
ISSN 1799-4934 (printed)
ISSN 1799-4942 (pdf)
http://urn.fi/URN:ISBN:978-952-60-4892-5

Unigrafia Oy
Helsinki 2012

Finland

441 697
Printed matter

Aalto University

Abstract

Aalto University, P.O. Box 11000, FI-00076 Aalto www.aalto.fi

Author
Huynh Van Khang

Name of the doctoral dissertation
Resistive Loss Modelling for Inverter-fed Induction Motors

Publisher School of Electrical Engineering

Unit Department of Electrical Engineering

Series Aalto University publication series DOCTORAL DISSERTATIONS 162/2012

Field of research Electromechanics

Manuscript submitted 10 August 2012 **Date of the defence** 21 December 2012

Permission to publish granted (date) 25 October 2012 **Language** English

☐ **Monograph** ☒ **Article dissertation (summary + original articles)**

Abstract

The aim of this research is to model resistive losses in induction motors. The resistive losses in the form-wound stator windings of induction motors were modelled by using time-discretized finite element analysis (FEA) and circuit models. Loss modelling with a high level of accuracy by means of FEA can be used in the demanding design of electrical machines, typically for high-power and high-speed induction motors in spite of its high computational cost. Alternatively, the equivalent circuits served as a cheap computational tool for the rapid estimation of the resistive losses of 37-kW and 1250-kW machines for motor drives without using the machine data, typically the machine structure and materials.

Electromagnetic losses lead to a temperature rise in electrical machines. As a result, temperature rise analysis is required to check whether the induction motors that are designed fulfill the IEC standard or design constraints. Thermal analysis employs FEA or a thermal network depending on the specific problems being studied. In this study, Finite Element Method Magnetics - a public domain code - was used to analyse the temperature rise of the form-wound stator windings of a 1250-kW induction motor. The thermal network was used in the thermal analysis of a 300-kW high-speed motor using form-wound stator windings. After the loss and thermal information have been collected, the losses in the stator form-wound windings of the induction motors are minimized in collaboration with temperature rise checking in the design stage. In addition, the loss and temperature rise analysis may offer numerical data to evaluate the possibility of using the form-wound windings for high-speed induction motors.

Keywords Resistive loss, eddy-current loss, equivalent circuit, co-simulation, loss minimization

ISBN (printed) 978-952-60-4891-8 **ISBN (pdf)** 978-952-60-4892-5

ISSN-L 1799-4934 **ISSN (printed)** 1799-4934 **ISSN (pdf)** 1799-4942

Location of publisher Espoo **Location of printing** Helsinki **Year** 2012

Pages 110 **urn** http://urn.fi/URN:ISBN:978-952-60-4892-5

Symbols

The underlined symbols are complex-valued quantities.

A_{ew1}	end-winding cooling area [m^2]
B_{12}, B_{11}	width of a stator slot [m]
b_{ss}	width of a slot insulation in the random-wound winding [m]
D	cross-sectional diameter of a coil [m]
D_{12}	inner diameter of the stator core [m]
D_{c}	cross-sectional diameter of the conductor in the coil [m]
D_{wo}	end-winding outer diameter [m]
H_1	height of a stator slot [m]
H_{13}	height of conductor part in a stator slot [m]
h	heat transfer coefficient [W/(m^2K]
h_{ad}	additional height between two winding layers [m]
h_{c}, h_{sc}	height of a conductor bar [m]
h_{ib}	height of a bar insulation [m]
h_{sb}	distance from the top bar to the air gap [m]
$\underline{i}_{\mathrm{est}}$	stator current estimated from the equivalent circuit in Figure 3.8 [A]
$\underline{i}_{\mathrm{r}}$	total rotor current [A]
$\underline{i}_{\mathrm{r1}}^{\mathrm{k}}$	rotor current of the first branch in general reference frame [A]
$\underline{i}_{\mathrm{r2}}^{\mathrm{k}}$	rotor current of the second branch in general reference frame [A]
$\underline{i}_{\mathrm{r3}}^{\mathrm{k}}$	rotor current of the third branch in general reference frame [A]
$\underline{i}_{\mathrm{s}}$	stator current [A]
$\underline{i}_{\mathrm{s}}^{\mathrm{k}}$	stator current in general reference frame [A]
L_{e}	self-inductance resulting from eddy current effect [H]
L_{m}	magnetizing inductance [H]
L_{r1}	self-inductance of the first branch [H]
L_{r2}	self-inductance of the second branch [H]
L_{r3}	self-inductance of the third branch [H]
$L_{\sigma\mathrm{s}}$	stator leakage inductance [H]
l_{end}	coil length outside the form-wound stator [m]
$l_{\mathrm{end-r}}$	coil length outside the random-wound stator [m]
N_1	number of coils in a slot
N_{s}	number of stator slots
P_{st}	stator resistive loss of the motor [W]
P_{rt}	rotor resistive loss of the motor [W]
P_{t}	total resistive loss of the motor [W]

p_{loss} power loss density [W/m^3]

R_9 upper convection thermal resistances [K/W]

R_{10} lower convection thermal resistances [K/W]

R_{e} resistance resulting from eddy current effect [Ω]

R_{ew1} axial thermal resistance in the end-winding region [K/W]

R_{ew2} radial thermal resistance in the end-winding region [K/W]

R_{r} total rotor resistance [Ω]

R_{r1} rotor resistance of the first branch [Ω]

R_{r2} rotor resistance of the second branch [Ω]

R_{r3} rotor resistance of the third branch [Ω]

R_{s} stator resistance [Ω]

R_{sw1} radial thermal resistance [K/W]

R_{sw3} tangent thermal resistance [K/W]

T temperature [K]

T_0 ambient temperature [K]

T_{e} electromagnetic torque [Nm]

$\underline{u}_{\mathrm{r}}$ rotor voltage [V]

$\underline{u}_{\mathrm{s}}$ stator voltage [V]

$\underline{u}_{\mathrm{s}}^{\mathrm{k}}$ stator voltage at general reference frame [V]

w_{ib} width of a bar insulation [m]

w_{is} width of a slot insulation [m]

w_{sc} width of a conductor bar [m]

Z_{c1} end-ring impedance of the first branch [Ω]

Z_{c2} end-ring impedance of the second branch [Ω]

$\underline{Z}_{\mathrm{e}}$ the small-signal impedance of the motor in the stator reference frame [Ω]

Z_{ie} imaginary part of impedance from the circuit [Ω]

Z_{im} imaginary part of impedance from the FEA data [Ω]

Z_{re} real part of impedance from the circuit [Ω]

Z_{rm} real part of impedance from the FEA data [Ω]

Δ a small-signal perturbation of a variable

λ thermal conductivity [W/(m.K)]

λ_{w} thermal conductivity of conductor [W/(m.K)]

$\underline{\psi}_{\mathrm{s}}$ stator flux linkage [Wb]

$\underline{\psi}_{\mathrm{r}}$ rotor flux linkage [Wb]

$\underline{\psi}_{\mathrm{s}}^{\mathrm{k}}$ stator flux linkage at general reference frame [Wb]

$\underline{\psi}_{\mathrm{r1}}^{\mathrm{k}}$ rotor flux linkage of the first branch at general reference frame [Wb]

$\underline{\psi}_{\mathrm{r2}}^{\mathrm{k}}$ rotor flux linkage of the second branch at general reference frame [Wb]

$\underline{\psi}_{\mathrm{r3}}^{\mathrm{k}}$ rotor flux linkage of the third branch at general reference frame [Wb]

ω_{k} angular frequency at general reference frame [rad/s]

Abbreviations

2D, 3D	two-dimensional, three-dimensional
ac	alternating current
dc	direct current
DC. Res. Loss	dc resistive loss
DE	differential evolution
FE	finite element
FEA	Finite Element Analysis
FEMM	Finite Element Method Magnetics - public domain code
FRF	frequency response function
GA	genetic algorithm
PAM	pulse amplitude modulation
PI	proportional integral
PSO	particle swarm optimization
PWM	pulse width modulation
rms	root mean square
sin	sinusoidal
Total. Res. Loss	total resistive loss

Preface

The dissertation was carried out from September 2008 to August 2012 at the Department of Electrical Engineering, Aalto University.

I would like to express my gratitude to Professor Antero Arkkio for his guidance, support and valuable comments during the research. The instructions from Dr. Anna-Kaisa Repo at the beginning of the research work and her constant help are fully appreciated. I wish to thank Dr. Juha Saari from Ingersoll Rand and Dr. Mohammad Jahirul Islam from ABB Sweden for their expertise and comments on the papers.

I also thank the Head of Department, Prof. Asko Niemenmaa, Docent Annouar Belahcen, Emeritus Prof. Tapani Jokinen, and Dr. Marko Hinkkanen for their encouragement, discussions and cordiality. Paavo Rasilo and Ari Haavisto have supported me in my daily and research life. Other colleagues, Emad , Kati, Jenni, Javi, Illari and Anssi, helped to create a warm working environment.

Financial support was given by the Academy of Finland, the Graduate School of Electrical Engineering of Aalto University, CIMO, and the Ingersoll Rand company. In addition, personal scholarships were provided by the Fortum Foundation, the Finnish Cultural Foundation, the Association of Electrical Engineers in Finland (SIL) and the Walter Ahlstrom foundation.

Special thanks to my wife, Hien, and my sons, Tommi - Quang and Leo - Vinh, for their love and smiles. I am deeply grateful to my parents, my brother Thach, and my sisters Thuy and Linh for their encouragement and care.

Contents

List of Publications

This thesis consists of an overview and of the following publications.

I Huynh Van Khang, Anna-Kaisa Repo, Antero Arkkio. Resistive Loss Identification of an Inverter-Fed Deep-Bar Induction Motor. *IEEE International Symposium on Power Electronics, Electrical Drives, Automation and Motion*, pp. 105 - 110, June 2010.

II Mohammad Jahirul Islam, Huynh Van Khang, Anna-Kaisa Repo, Antero Arkkio. Eddy-Current Loss and Temperature Rise in the Form-Wound Stator of an Inverter-Fed Cage Induction Motor. *IEEE Transactions on Magnetics*, Vol. 46, No. 8, pp. 3413 - 3416, August 2010.

III Huynh Van Khang, Antero Arkkio. Parameter estimation for a deep-bar induction motor. *IET Electric Power Applications*, Vol. 6, No. 2, pp. 133 - 142, February 2012.

IV Huynh Van Khang, Antero Arkkio. Eddy-Current Loss Modeling for a Form-Wound Induction Motor using Circuit Model. *IEEE Transactions on Magnetics*, Vol. 48, No. 2, pp. 1059 - 1062, February 2012.

V Huynh Van Khang, Antero Arkkio, Juha Saari. Loss Minimization for Form-wound Stator Winding of a High-Speed Induction Motor. *accepted, IEEE Transactions on Magnetics*, 6 pages, 2012.

Author's Contribution

Publication I: "Resistive Loss Identification of an Inverter-Fed Deep-Bar Induction Motor"

The paper was written by Huynh Van Khang. Dr. Anna-Kaisa Repo and Prof. Antero Arkkio have contributed with suggestions, comments and their expertise concerning FEA and the estimation method.

Publication II: "Eddy-Current Loss and Temperature Rise in the Form-Wound Stator of an Inverter-Fed Cage Induction Motor"

The paper was first written by Huynh Van Khang. Dr. Mohammad Jahirul Islam modified some paragraphs of the paper. The FEA code for modelling eddy-current losses was developed by Dr. Mohammad Jahirul Islam. Huynh Van Khang used the code to calculate the losses and implement FEMM for temperature rise analysis. Prof. Antero Arkkio and Dr. Anna-Kaisa Repo contributed with suggestions, comments, and their expertise concerning FEA.

Publication III: "Parameter estimation for a deep-bar induction motor"

The paper was written by Huynh Van Khang. Prof. Antero Arkkio contributed with suggestions, comments, and his expertise concerning FEA and measurements.

Publication IV: "Eddy-Current Loss Modeling for a Form-Wound Induction Motor using Circuit Model"

The paper was written by Huynh Van Khang. Prof. Antero Arkkio contributed with suggestions, comments, and his expertise concerning FEA.

Publication V: "Loss Minimization for Form-wound Stator Winding of a High-Speed Induction Motor"

The paper was written by Huynh Van Khang. Prof. Antero Arkkio has contributed with suggestions, comments, and his expertise concerning FEA. Dr. Juha Saari contributed with comments, and his expertise concerning thermal analysis.

1. Introduction

1.1 Background

Inverter-fed electrical machines are widely used in industrial sectors. They operate at high efficiency when supplied by frequency converters. However, even a minor improvement in their performance would significantly reduce the transferred energy losses. The magnitude of these losses can be greatly affected during either the design or use stages of the electrical machines. Within the design process, a machine can be structurally optimized to reach the minimum losses. For end users, optimal controls reduce the losses in the machines. In both approaches, the modelling and optimization of electromagnetic losses in electrical machines remain extremely demanding.

Computational methods for modelling electrical machines have been developing explosively for many decades. Their applications range from designing to controlling electrical machines. Among these methods, finite element analysis (FEA) has served as a powerful tool to model complicated phenomena in electrical machines, for instance, eddy-current or saturation problems. The collection of sufficient information from the modelling supports the optimization process in the design stage. However, FEA modelling requires detailed data on electrical machines, and it is time-consuming. Being a faster tool, circuit models are a simple method to predict losses in electrical machines. During the use stage, for instance in motor drives, a controller usually communicates with an electrical machine via a circuit model representing the machine. The PI gains of the current controller are calculated from the electrical parameters and system bandwidth. Appropriate circuit models for the machines allow the drive systems to operate at their highest performance levels. Moreover,

optimal controls use the parameters to define electromagnetic losses and torque via analytical functions.

Electromagnetic losses, typically resistive and core losses, lead to a temperature rise in electrical machines. Thermal analysis is a prerequisite in any design of electrical machines. Temperature constraints are also stated in the international standards. Therefore, temperature rise analysis and electromagnetic modelling cooperate in the design stage. FEA is a tool for accurate thermal analysis. The optimization of an electrical machine requires up to thousands of thermal calculations. Thermal networks, a simpler and faster model compared to FEA, seem to be a suitable tool for checking the temperature rise constraints in the optimization in the design stage.

To reduce the electromagnetic losses, contemporary optimizations of electrical machines mainly concentrate on an optimal structure for the machine rotor. The machine stator using traditional random-wound windings costs less and is assumed to be optimal. However, the challenges involved in the modelling of the eddy currents in random-wound windings may cause an underestimation of the stator losses in the design stage. Contrary to random-wound windings, form-wound windings made of rectangular conductors have robust structures and high reliability, but they are expensive. The resistive losses in form-wound windings have been well modelled in the recent research. The good design of the machines is assisted by sufficient information being obtained from the modelling. In specific applications, such as high-speed machines for air compressors or gas pumps for undersea use, the savings resulting from reliable operation outweigh the initial investment costs. The cost will be further reduced by a minimum loss design for the stator form-wound winding.

Loss minimization in machine designs, a main objective of the modelling of electrical machines, normally involves optimizations and constraint checking. If the problem has many variables, the optimization will consume a lot of time. It is necessary to eliminate unimportant variables from the optimization to reduce the design cost. For the same purpose, the design constraints, for instance, thermal constraints, should be checked rapidly for a possible solution during the optimization.

1.2 Aim of the work

The main objective of this study is to model the resistive losses of induction motors in the design and control stages, taking the interaction of frequency converters into account. A sub-task is to develop a method to reduce the losses in electrical machines. To obtain sufficient loss information in the design stage, time-discretized FEA is used to model the resistive losses in form-wound induction machines. On the basis of a temperature rise, the structure of the form-wound stator windings is adjusted to reduce the resistive losses, and in order to fulfill the IEC-standard (IEC 60034-1 2004). To achieve fast modelling, equivalent circuit models are proposed and identified to model the resistive losses in electrical machines. The parameters of the circuit are estimated over a wide range of frequencies for applications in inverter-fed motors. Alternatively, the parameters of a deep-bar induction machine are estimated from the measured stator voltages and currents in the time domain without using information on the structure and materials of the motor.

1.3 Scientific contribution

This section presents the scientific contributions extracted from Publications I to V.

It was found that the resistive losses are dependent on the harmonic amplitudes and independent of the harmonic phases. Other than an appropriate circuit model representing an induction motor, the loss prediction for the motor does not require additional circuits to take the higher harmonic effects into account.

A method to estimate the parameters of a triple-cage circuit in the time domain is developed by using differential evolution. When the parameters of the circuit are accurately estimated, the triple-cage circuit well represents a deep-bar induction motor in both the steady and transient states.

An equivalent circuit for modelling the resistive loss in a form-wound induction motor is proposed. The eddy-current losses in form-wound induction machines can be taken into account by adding extra circuit branches to the T-equivalent circuit. A comparison of the performance evaluations between the circuit model and time-discretized FEA shows a good agreement with errors of less than 3 %.

Sufficient information on the losses, combined with temperature rise analysis, is required in order to have a good design for the form-wound winding of a high-power motor based on the IEC standard (IEC 60034-1 2004). It was shown that the hottest spot in a form-wound stator is the bar closest to the air-gap. When the distance from the stator bar to the air-gap is increased, the resistive losses are reduced.

A co-simulation model is developed by combining an optimization and a thermal network in Matlab and time-discretized FEA. The model is used to minimize the resistive loss in the stator winding of a high-speed induction motor. The resistive losses in the stator are reduced by about 10 % within certain limits of stator dimensions and temperature rise.

It was shown that the Taguchi approach (Roy 2001) can be used as an optimization method for minimizing torque ripple in electrical machines or for other purposes. To minimize the resistive losses in form-wound stator windings, the approach cannot serve in that manner if the eddy-current effects are taken into account. However, it can be used to determine which parameters are important for minimizing the resistive losses. On the other hand, it helps to reduce the computational cost of the loss minimization.

If eddy-current loss in the form-wound stator windings of high-speed induction motors is to be minimized, it is important to consider the type of the voltage supply. Depending on the voltage supplies, the optimization tries to reduce or compromise between dc-resistive and eddy-current losses in the stator winding.

1.4 Structure of the dissertation

The work is organised into 4 chapters. Chapter 1 introduces the background, motivation, and objective of the dissertation. The scientific contribution and accepted publications related to the work are listed at the end. Chapter 2 reviews up-to-date research in the literature related to resistive loss modelling, parameter estimation, thermal analysis and optimization of electrical machines. Chapter 3 summarizes the methods and main results that have been presented in the publications. Chapter 4 introduces some discussions and conclusions.

1.5 Overview of publications

The publications are summarised in this section as follows

Publication I

The effect of pulse width modulation (PWM) supply on the resistive loss is studied for induction motors with a rated power of 45 kW and 1250 kW. It can be seen from the Fourier decomposition of a classic 4 kHz inverter supply that the 5th (250 Hz) harmonic and 79 th (3950 Hz) harmonic voltages have the dominant amplitudes, and typically represent for low and high frequency ranges of harmonics. These are superimposed on the fundamental voltage to study the effects of the harmonic amplitude and phase on the resistive losses of the motor. From the results of time-discretized FEA, it is clear that the resistive losses are independent of the harmonic phases, and proportional to the square of the harmonic amplitudes. The behaviour of those machines seems to be a linear system at high order harmonics. Within this work, the parameters of a triple-cage circuit representing a deep-bar induction machine are estimated using the impulse method (Repo 2008). The resistive losses calculated from the circuit are compared to the losses calculated by the time-stepping FEA. The estimation method is based on the transfer function in the frequency domain, so the machine was required to be linearized within a certain frequency range. The impulse method needs the estimation data of voltages and currents from small excitation to be less than 10% of the fundamental voltage.

Publication II

The eddy-current losses in the form-wound windings of high-power induction machines were successfully modelled by Jahirul Islam (2010). The eddy-current losses in a form-wound stator winding fed by a frequency converter serve as the input for a temperature rise analysis using the public domain code FEMM. The inhomogeneous distribution of the eddy-current losses produces different hot spots in the stator windings. The hottest spot is the top bar closest to the air-gap, and the coldest spot in the stator winding is the innermost slot bar. However, the standard IEC 60034-1 proposes that the difference between the maximum temperature and average temperature should be below 10 K. The distance from the top bar to the air-gap has to be adjusted to reduce the eddy-current losses in the form-wound stator winding, and then the machine being studied

matches the qualification of the standard.

Publication III

To overcome the difficulty of using the estimation method in Publication I, a method for estimating the parameters of the triple-cage circuit representing a deep-bar induction motor in the time-domain is proposed. The data for the estimation consist of the stator voltages, currents and speed. These can easily be measured by research groups or industry. The parameters are estimated both in the steady state and transient state by a curve-fitting technique using differential evolution. The estimation method was verified by a comparison of the machine performances evaluated by the circuit model and an existing tool - FEA. The variation in the parameters related to the slotting harmonics in a non-skewed deep-bar induction motor was shown in the study. The constant parameters of the triple-cage circuit well represent the motor in the transient state when the motor is started.

Publication IV

For a faster and simpler model to take the eddy-current effects into account, a circuit model was developed in this study. From the inhomogeneous distribution of resistive losses in the form-wound stator windings, it was clear that a dc resistance is not sufficient to represent the ac resistive losses in form-wound induction motors. The T-equivalent circuit is modified by adding extra branches. The purpose is to increase the order of impedance frequency response. The augmented circuit can take the eddy-current effects into account. The total resistive losses calculated from the circuit are compared to those from the time-discretized FEA in Publication II to verify the feasibility of the proposed circuit.

The parameters of the circuit are estimated over a range of frequencies (-200 to 200 Hz) so as to adapt any direction of the rotation as referred to the stator reference frame. This allows the circuit parameters still to remain valid for the higher harmonics from the frequency-converter supplies. The data for parameter estimations are collected from FEA.

Publication V

To achieve a better performance for a high-speed induction motor using form-wound stator windings, a loss minimization is required to improve the performance of the form-wound stator windings. The electromagnetic

losses are modelled by means of time-discretized FEA. It is quite time-consuming if all the stator dimensions are varied in the optimization using data from the time-discretized FEA. To reduce the time consumption, some dimensions should be omitted in the optimization if their effects on the electromagnetic losses are small. The Taguchi approach is used to analyse the effects of the variables on the electromagnetic losses. From this evaluation, the number of variables for the optimization is determined.

The supplies for the motor during optimization using differential evolution (DE) are pure sinusoidal and pulse amplitude modulation - PAM. With the pure sinusoidal supply, the optimization reduces mainly dc resistive losses when it increases the cross-sectional area of the copper bars. The optimization with the PAM supply reduces the eddy-current losses by increasing the distance from the top bar to the air-gap.

2. Review of Relevant Research

Up-to-date research related to the work is reviewed in this chapter. The modelling methods for predicting the resistive losses in electrical machines will be summarised from the point of view of modelling tools, typically FEA and circuit models. Thermal modelling related to the electromagnetic losses will follow next. Finally, optimization algorithms to reduce the losses in electrical machines will be reviewed.

2.1 Modelling of resistive losses by finite element analysis

In general, resistive losses are the largest losses in electrical machines. Since the beginning of FE modelling for electrical machines, stator resistive loss has normally been modelled by a lumped dc resistance (Arkkio 1987). However, the dc resistances can only model the dc resistive losses or homogeneously distributed losses in electrical machines. Therefore, this cannot be an appropriate solution for modelling eddy-current losses in the copper area of electrical machines.

In modern electric drives, electrical machines are fed by frequency converters. It is necessary to take the losses of electrical machines under multi-harmonic voltages into account (Yamazaki and Watari 2005), (Yamazaki et al. 2009). The loss distribution of inverter-fed electrical machines was considered by Lee et al. (2004) and Liu et al. (2008). To study the effect of PWM supply on the electromagnetic losses in the motor, the authors used time-stepping FEA. The difference between the losses caused by purely sinusoidal and PWM supplies was shown in Lee et al. (2004). The important role of sufficient loss information in the design stage was mentioned in the same research. In the report, dc resistance stands solely for the resistive losses in the stator winding of an induction motor. That means only the dc resistive loss in the stator winding.

Lähteenmäki (2002) calculated the electromagnetic losses in high-speed induction machines by using FEA. The measurements in the research showed the difference between the measured and calculated losses to be about 20%. The reason for this phenomenon is that the FEA modelling did not take all the losses in the machines into account. Circulating current losses and extra power losses were mentioned as the main problems in the study. The role and selection of power supply for high-speed machines were also discussed in the report.

To predict the losses of an electrical machine in its design stage sufficiently well, Jahirul Islam et al. (2007) modelled stator resistive losses in the form-wound stator winding of an induction motor using 2D time-harmonic FEA. The stator resistive losses consist of the dc resistive loss and eddy-current loss. The effects of magnetic saturation and nonlinearity were taken into account in the time-harmonic FEA. Time-harmonic FEA is time-efficient, but it is not suitable for modelling the losses in inverter-fed motors. To include higher harmonic effects, Jahirul Islam and Arkkio (2009) presented time-stepping FEA to calculate the stator resistive losses in a high-power induction motor. Time-stepping FEA successfully modelled the eddy-current losses when the motor was supplied by a PWM voltage. As a consequence, time-stepping FEA rather than time-harmonic FEA seems to be an appropriate solution for modelling the resistive losses in electrical machines under inverter interactions.

In another approach, Gyselinck et al. (2010) modelled the eddy-current losses in the form-wound stator winding using frequency- and time-domain homogenization methods. FEA was used to take the skin and proximity effects into account before the homogenization technique was used. The resistive losses are computed in both the frequency domain and time domain. The eddy-current loss from a PWM supply modelled by FEA requires sufficiently detailed finite elements. One more degree of freedom of the homogenization technique is needed for an accurate calculation of the eddy-current losses. The tools for the accurate calculation of the losses are expensive, but they are necessary for designing high-performance machines.

The importance of resistive loss modeling means that it is still an attractive topic for extensive research (Amara et al. 2010, Lubin et al. 2010, Wu et al. 2012, Yamazaki et al. 2012). Stermecki et al. (2012) and Wrobel et al. (2012) developed 3D FEA to take the eddy-current effects into account. The development of processors in recent years has allowed re-

searchers to use 3D simulation for accurate calculation Lin (2010). The additional losses of inverter-fed induction motors are shown in this report. The research using 3D simulation rather focus on the eddy-current losses in the structural parts and the end-winding than in the core region, where 2D FEA can well manage the loss prediction.

In brief, time-stepping FEA is recognized as an accurate tool for modelling the resistive losses in the copper areas of inverter-fed electrical machines. Unfortunately, it is very time-consuming. In the design stage of electrical machines, it may require up to thousands of FEA simulations. The reduction of the time consumption involved in using the time-stepping FEA remains a challenge.

2.2 Circuit modelling of electrical machines

Circuit models are an alternative option for modelling electromechanical devices (Yamazaki 2002, Laldin et al. 2011). The modelling using the circuit model is not as accurate as FEA, but it significantly reduces the time consumption of the modelling. In addition, it is not necessary to know the motor structure and materials in detail. In a recent report, Li et al. (2010) developed an adaptive circuit to model a Thomson-coil actuator. Each segment of the coil is modelled by an RL circuit to take the eddy-current effect into account. The circuit model seems to be a promising approach simplifying the modelling of electromagnetic phenomena in electrical machines.

In motor drives, circuit models are representatives of electrical machines in the control systems. Within a drive scheme, the outputs of the PI current regulators are reference voltages for inverters as in the analysis by Briz et al. (2000). The PI gains of the current regulator are calculated from its bandwidth and the electrical parameters of the machines. The motor manufacturers normally provide electrical parameters of T-equivalent circuits at rated operating points. However, the users control the motors at different operating points. The effect of motor parameters on the motor performance was recently shown by Hwang et al. (2010). The use of incorrect parameters may damage the performance of inverter-fed motors.

Using the same approach, Sudhoff et al. (2002) mentioned the problem of traditional d-q equivalent circuits for inverter-fed electrical machines. The d-q circuit can only predict the fundamental current and average torque. The circuit model in motor controls should be adaptive. The au-

thors proposed an induction motor model to study the interaction between the inverter system and the motor. The model can take the saturation effects into account by assuming the linkage fluxes as a function of currents. The model was built up into integrated and complicated functions. To apply the model in a specific application, Sudhoff et al. (2003) simplified the model into small-signal impedance and a steady-state equivalent circuit. The model was well capable of representing the motor fed by an inverter in predicting stator currents and torque ripple. However, the loss prediction based on the circuit and the influence of the phase and amplitudes of higher harmonics has not been studied yet. Although the procedure to estimate the parameters for those circuits is still a challenging task in experiments, those studies confirmed that the improvement of circuit models under the effects of frequency converters is necessary for energy-efficient electric drives.

Methods to estimate the parameters have recently been proposed as an effort to improve the electric drive performance. From a motor structure, Dolinar et al. (1997) and Stumberger et al. (1998) used FEA to calculate the parameters for two-axis models of induction motors. In the same approach, Stumberger et al. (2001) paid more attention to the saturation and magnetization under load conditions. Those methods required motor information, typically structure and material, in the design stage. To take the skin effect in a deep-bar induction motor into account, Repo et al. (2006) introduced a distributed circuit representing the motor. The parameters of the circuit were predicted by time-harmonic FEA. For electric drives, Stumberger et al. (2004) and Sonnaillon et al. (2007) introduced experimental methods to estimate a few parameters from the circuits represented for electrical machines. Recently, Repo (2008) presented dynamic induction-motor models for motor controls. Estimation methods using an impulse test and FEA were used to predict a large number of parameters over a wide range of frequencies. The transfer functions in those studies are suitable for the linear system in the frequency domain, as explained by Harnefors (2007) and Hinkkanen et al. (2010). In brief, the limited parameters of a T-equivalent circuit may be experimentally identified in the time domain as shown in the literature (Stumberger et al. 2004). For a large number of parameters in the circuit, the motor is normally linearized in the frequency domain for the estimation. In up-to-date research, there is a lack of methods in the literature to estimate a large number of motor parameters in the time domain.

Bazzi and Krein (2010) reviewed up-to-date methods for minimizing the losses in inverter-fed electrical machines. Almost all loss-minimization algorithms have used parameters from the equivalent circuit to calculate the electromagnetic losses. The inclusion of the stray-load losses on the circuit model was studied by Boglietti et al. (2010). Additional resistance in series with the stator impedance can model the effects of air-gap spatial harmonics. The accuracy of the parameters is important for defining the electromagnetic losses for loss-minimization and improving the performance of electric drives. For the same purpose, Boglietti et al. (2011) presented computational algorithms to predict the electrical parameters of induction motors after designing a machine. It was necessary to have the structure and material information of the machine for the estimation. Gieras and Saari (2012) proposed a method to evaluate the performance of high-speed induction machines that was also based on the electrical parameters, using machine data available at the design stage. So far, the eddy-current loss has been treated as negligible by assuming a single dc resistance on the stator side. Anyway, the inclusion of the eddy-current loss in the circuit model is still lacking.

2.3 Thermal analysis of electrical machines

The limit of the power and torque of an electrical machine normally depends on the temperature rise constraints (Hafiz et al. 2010, Borisavljevic et al. 2010, Kolondzovski et al. 2011). Thermal analysis has become a must in machine designs, especially for high-speed machines (Huang et al. 2012). Therefore, there is a lot of research in the literature related to thermal analyses. This can be divided into two common groups based on the tools used to analyze temperature rises: FEA and thermal networks. FEA gives accurate results for temperature rises, but its time-consumption and cost are quite high. The thermal network is a cheaper tool, but it requires experience to define all the model parameters. Depending on their specific purposes, researchers should compromise between accuracy and cost.

Saari (1998) presented a thermal network for analyzing the temperature rises in high-speed machines. The model was validated by measurements. The lumped resistances within the thermal network were calculated from the dimensions of the motor. The maximum power of the motor was estimated on the basis of the thermal limitation. The model analyzed the temperature rise in induction machines that had random-wound sta-

tor windings. However, it was hard to find a study in the literature that specifies temperature rise analysis in form-wound electrical machines using thermal networks.

For greater accuracy, Inamura et al. (2003) used FEA to calculate the core and resistive losses in switched reluctance machines. The temperature rise was analyzed from the calculated losses. Good agreement with the measurements was shown in the report. The same approach to this kind of motor was presented by Faiz et al. (2009). This latter report, using the ANSYS commercial code calculated the electromagnetic losses in detail. The eddy-current loss in the stator winding was studied by an analytical model. The effects of the dimensions of the machine on the electromagnetic losses and temperature rise were mentioned in that study.

The evolution of temperature rise analysis was well summarized by Boglietti et al. (2009a). The authors evaluate the merits and demerits of temperature analyses using FEA and thermal networks. The cost of those approaches was visibly estimated. Heat-transfer coefficients for thermal networks need to be carefully determined as shown by Jankowski et al. (2010) and Bracikowski et al. (2012), while convection boundaries are important when using FEA (Hettegger et al. 2012). It seems that the use of FEA to model the temperature rise is suitable for modelling solid conduction components. In a later report, Boglietti et al. (2009b) developed a method to calculate heat-transfer coefficients for a thermal network, because of to its important role, as mentioned before. Huang et al. (2009) employed both 3-D FEA and thermal network in their thermal analysis of high-speed motors. These authors also mentioned the speed and cost of each method in the report. The modelling of electromagnetic losses used for a thermal network is a demanding task in the study by Zhao et al. (2011). Loss calculation using FEA may guarantee the accuracy of thermal analysis using thermal networks. All the thermal studies mainly focus on improvement of the modelling itself. It is difficult to find any reports in the literature combining thermal analysis with a design standard.

In a simple thermal problem, the temperature rise can be analyzed by using a public domain code like FEMM (Meeker 2009). The boundary conditions can be simplified on the basis of the code instruction. In a design process, to reduce the time consumption for the machine design, thermal constraints can be checked by a thermal network. The heat transfer coefficients of the thermal network have to be well defined and validated

beforehand. Traditionally, the electromagnetic losses can be accurately predicted by FEA for a temperature rise analysis.

2.4 Optimization of electrical machines

Accompanying the development of processors, optimizations have become a powerful tool to reduce the engineering costs. Modern optimization techniques for electrical engineering were reviewed and explained in a report by Lee and El-Sharkawi (2008). For design tasks, the optimization of electrical machines was focused on structural optimizations, as shown in the reports by Uler et al. (1995) and Centner and Schafer (2010). In a recent overview, Di Barba (2011) provided a good summary of the up-to-date optimization methods for electrical machines in the literature. For a fast design, the analytical functions are normally used to define the objective functions (Gao et al. 2010). FEA is an accurate tool for defining the objectives (Yamazaki 2010), but it is expensive. In principle, each optimization method has its own merits and demerits. It also depends on the applications and tools available within the research group. This issue is beyond the scope of this thesis. Naturally, electrical engineers select a method that is suitable from their point of view.

In an application of the optimization, Kim et al. (2009) used a magnetic equivalent circuit and FEA to design an interior permanent magnet synchronous motor. To ensure a highly accurate design, FEA was used in spite of its high cost. The Taguchi approach was the optimization method used in this study. Using the same approach, Islam et al. (2011) minimized the torque ripple in the same kind of motor. It seems that the Taguchi approach is a commonly used method to reduce the torque ripple in permanent magnet motors. As disputed in the report by Ben-Gal (2005), this approach may rather reach a quality design than be an optimal design. However, the Taguchi approach can evaluate the effect of variables on the objective functions. Recently, the method was used in the analysis of the magnetic field, as shown in the report by Shi et al. (2012). It seems from recent research that the Taguchi method is not directly used for loss minimization, especially in form-wound stator windings. For an optimal design, Zhang et al. (2012) used a multi-objective optimization algorithm combined with FEA to obtain an optimal structure for the rotor of an induction motor. It seems that the researchers focused mainly on the structure optimization on the rotor side. The optimal status of stator sides

is not clearly mentioned in the literature. In addition, the optimal methods mostly improve the performance of the motor, typically the torque or electromagnetic losses, in such a way that they are separate from thermal constraints. The combination of FEA and thermal analysis in the design process remains a problem.

The results of an optimization process are normally defined on the basis of the stopping conditions of an algorithm. The algorithm can stop after the number of the iterations reaches its maximum value or the objective function is unchanged over a large amount of evaluations (Pham et al. 2011). Designers have to compromise between the time consumption and stopping conditions in the algorithm. To reduce the time-consumption of using heuristic optimizations and FEA, the number of variables in the problem has to be reduced. As a result, the size of population or the number of FEA simulations are reduced. On the other hand, the influence of variables on the objective function has to be empirically or methodically evaluated in advance.

Besides applications for machine designs, optimizations have also been involved in the researches related to parameter estimation. For instance, Repo (2008) used differential evolution to estimate the parameters of induction motors. The same optimization was used to identify the parameters of a hysteresis model in the report by Toman et al. (2008). It is clear that the optimizations are widely used in modelling and designing electrical machines, and they continue to show great potential in the development of electrical machines.

2.5 Conclusions

As shown in the literature, sufficient information on electromagnetic losses was necessary in both the design and control stages of inverter-fed electrical machines. In a specific problem of minimizing resistive losses, it is important to know which input data are required for a design process. Accurately calculated losses may guarantee the evaluation of the temperature rise or power limit of the machines.

It has been shown that the losses in the traditional random-wound windings were underestimated. This may cause a non-optimal design for a motor using random-wound windings. It was clear that the dc resistive loss is not the only loss in the stator windings. The eddy-current losses in the stator winding have to be sufficiently modelled to minimize the difference

between predicted and measured losses. For a highly reliable machine, the form-wound stator windings are probably a good option, especially in high-speed and high-power machines. In the optimization process of the form-wound stator winding, a co-simulation model consisting of FEA, thermal analysis, and an optimisation algorithm may be an interesting piece of work in the industrial design.

As a cheap tool for modelling in electric drives, circuit models can be further developed to take complicated phenomena in electrical machines into account. For instance, the T-equivalent circuit needs to be augmented to take the effect of the other losses into account by means of extra circuit branches. As a result, the number of parameters in the circuit is increased and it becomes more demanding to identify them correctly. Before the circuit model is developed, it is necessary to know the behaviour of harmonics on the machine performance.

Optimizations have been described as useful tools to reduce the cost of modelling and designing electrical machines. Those can be diversified into applications such as parameter estimation or machine design. In a design problem, as mentioned above, the application of the Taguchi approach in minimizing the resistive loss in the stator is not studied in the literature. In predicting a large number of circuit parameters in the time domain, an estimation model needs to be further developed by using an optimal algorithm.

3. Methods and results

The main objective of the work is to model and reduce the resistive losses in induction motors. The results of the work have been shown in the publications. In this section, the methods that were developed and the main results are summarized.

3.1 Resistive loss modelling using finite element analysis

The resistive losses in the form-wound stator winding of a 1250-kW induction motor were modelled by using time-discretized FEA as shown in Figure 3.1. As the eddy-current effect was taken into account, the total resistive loss in the stator is higher than the dc resistive loss (Publication II). The eddy-current loss is the difference between those resistive losses. More details of the eddy-current loss modelling can be found in Jahirul Islam (2010).

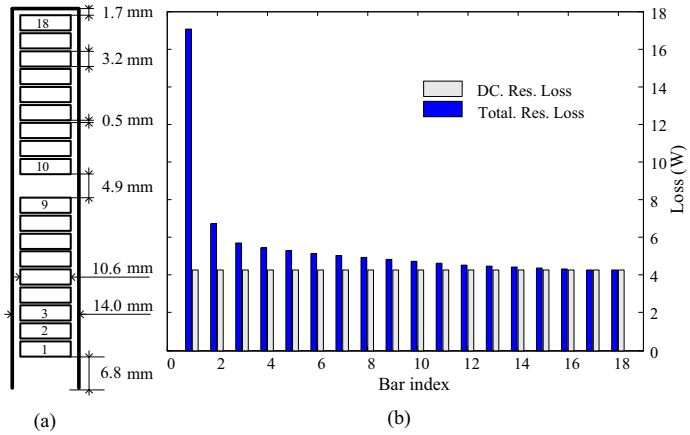

Figure 3.1. Stator winding (a) and its resistive loss distribution (b).

To reduce the eddy-current loss, magnetic slot wedges were used to close

the slot openings. The slot wedges reduce the ripples of the air-gap flux and the interaction of this flux on the conductors close to the air-gap. As shown in Figure 3.2, the eddy-current loss reduces when the distance from the conductors closest to the air-gap to the air-gap is increased. The loss is further reduced by using magnetic slot wedges.

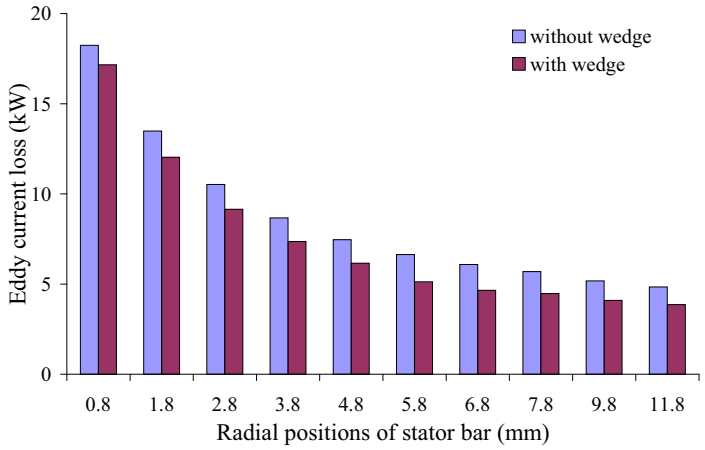

Figure 3.2. Variation of eddy-current losses with and without magnetic slot wedges at different radial positions.

In an application of time-discretized FEA, the resistive losses in a 300-kW, 60000- rpm HSIM using form-wound stator windings were calculated and reduced in the Publication V. Here, some details of the motor and assumptions are presented. Descriptions and figures of the motor using random-wound windings can be found in Gieras and Saari (2012). The basic parameters of the motor are presented in Table 3.1. The two-layer random-wound winding of the motor is shown in Figure 3.3 (a). The form-wound stator winding shown in Figure 3.3 (b) is designed on the basos ofthe original one. The cross-sectional area of the conductor and the height of the slot H_1 are kept the same between the two models.

In FEA modelling, the length of the end-winding of the form-wound stator winding is assumed to be the same as that of the random-wound winding. However, it is useful to discuss some possibilities concerning the end-winding model of the form-wound stator winding. Normally, the length of the end-winding is not a problem for multi-pole pair, high-power, form-wound motors because it is still within an acceptable range (Mesrobian and Holdrege 1990). Resistive losses will concentrate in the end-winding when the end-winding length is too long. If the same approach is applied for a 2-pole HSIM, the end-winding arrangement is shown in Figure 3.4.

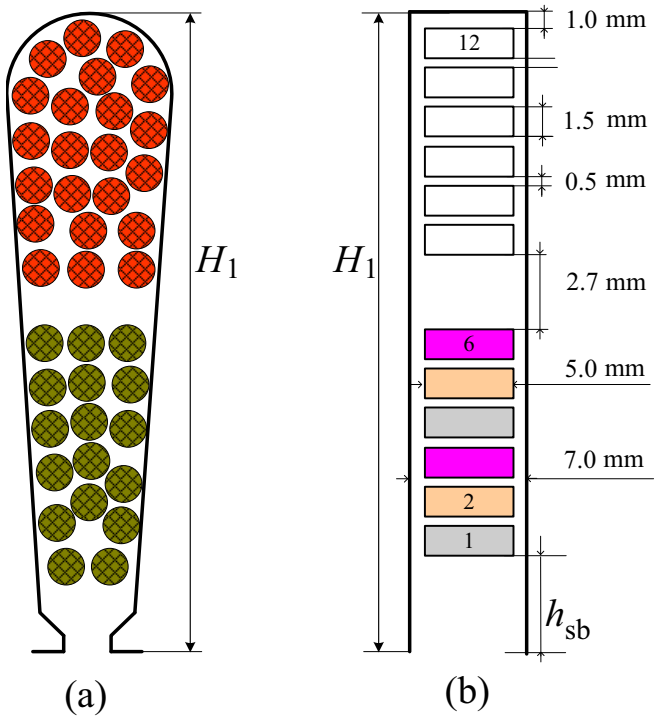

Figure 3.3. Random-wound stator slot (a) and form-wound stator slot (b).

If the width of each bar and the distance from bar to bar in the end region are w_c and w_{bb}, the shortest radial length of the end-winding is ($6w_c$ + $5w_{bb}$). As a result, the coil length of the end-winding is very long. This causes a large resistive loss in the end-winding. One way to reduce the end-winding length is that the coil-pitch of the stator windings should be reduced. However, an increase in the magnetizing current as a result of the smaller coil-pitch may lead to a greater loss in the motor.

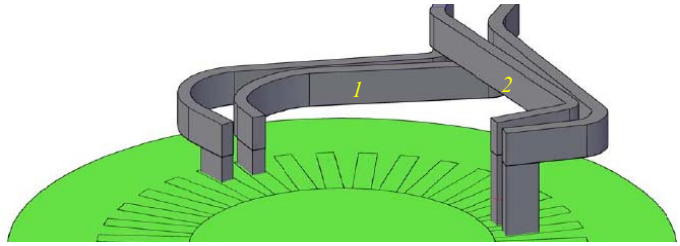

Figure 3.4. Two-plane end-winding model of form-wound winding.

The practical feasibility of the stator winding should be considered in the design stage. In principle, the form-wound coils are prepared in a form before they are arranged in the stator core. If the curvature length of the

Table 3.1. Data of studied HSIM.

Rated voltage (V)	400
Rated power (kW)	300
Number of stator slots	36
Rated slip (%)	1.0
Number of poles	2
Effective length (mm)	178
Inner stator core diameter (mm)	115
Outer stator core diameter (mm)	250
Outer rotor core diameter (mm)	109

end-winding is larger than the inner stator perimeter, it is impossible to put the end-winding into the stator core. To deal with those problems, a three-plane end-winding model is presented in Figure 3.5. It is possible to subdivide the 6 coils per phase into 3 coils per plane in the axial direction. The upper layer coils are arranged in Planes 1 and 2, while the lower ones are in Planes 2 and 3. For instance, within Plane 2 in Figure 3.5, the coils on the right-hand side (right-red) are in the lower layer of the stator slots, and the coils on the left-hand side (left-red) are in the upper layer of the stator slots. The right-red and left-red coils can be changed to the upper and lower layers in the stator slots by connecting them to the coils in Plane 1 and Plane 3, respectively. This model will be assumed in the thermal evaluation of the form-wound stator windings in this research.

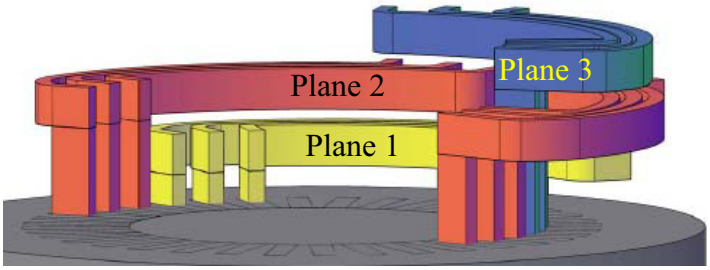

Figure 3.5. Three-plane end-winding model of form-wound winding.

The motor is studied in Publication V with two different power supplies: pure sinusoidal - sin and Pulse Amplitude Modulation - PAM - as shown in Figure 3.6. Pulse Width Modulation (PWM) was not a good supply for HSIMs as mentioned by Lähteenmäki (2002). The electromagnetic losses in the motor using form-wound windings with the sinusoidal and PAM supplies collected by FEA will be used in the optimization process.

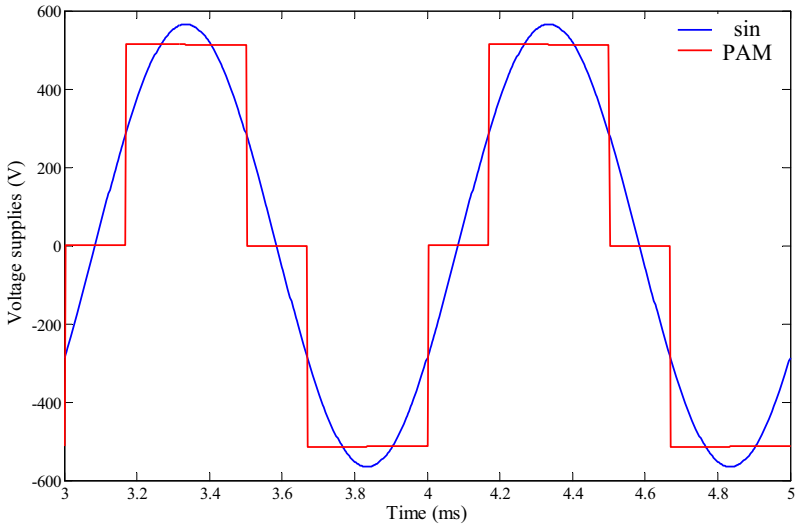

Figure 3.6. Voltage supplies for HSIM.

3.2 Resistive loss modelling using circuit models

As a faster and simpler tool for modelling, circuit models are an alternative option to predict the resistive losses of electrical machines. This section presents equivalent circuits of the machines, typically for medium- and high-power machines. The application of the circuit parameters to identify the resistive losses will follow estimation methods for the equivalent circuits.

An investigation of the effect of the amplitudes and phases of the PWM harmonics was shown in Publication I. The investigation of 45-kW and 1250-kW induction machines was carried by using time-stepping FEA. The 5th and 79th harmonics of a PWM supply were separately superimposed on the fundamental voltage of 50 Hz. When the harmonic amplitudes are increased from 5% to 40% those of the fundamental voltage, the stator and rotor resistive losses are quadratically increased. However, the stator and rotor resistive losses are independent of the harmonic phases when the phases are increased from 0 to $90°$. More details of the study can be found in that report. It was shown that there is no need to have additional circuits to identify the resistive losses at higher frequencies.

3.2.1 Resistive loss modelling for a deep-bar induction motor

A triple-cage circuit representing a deep-bar induction motor was introduced in Publication I and by Repo (2008). The reports presented methods

to estimate the parameters of the circuit by using FEA and the impulse method. The dimensions and materials of the motor were required for the estimation when using FEA. When the impulse method is being used, the machines have to be linearized because the parameters are estimated in the frequency domain using transfer functions (Harnefors 2007). Figure 3.7 shows the equivalent circuit of a 37-kW deep-bar induction motor (Publication III).

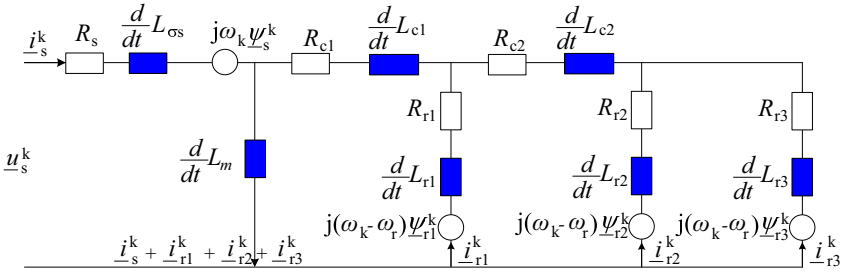

Figure 3.7. Triple-cage equivalent circuit.

Voltages, flux linkages, and currents were written in the space vector form. For instance, the stator voltage and flux can be written as in (3.1) and (3.2). The rotor voltages and flux equations can be found from Publication III.

$$\underline{u}_s^k = R_s \underline{i}_k^k + \frac{d\underline{\psi}_s^k}{dt} + j\omega_k \underline{\psi}_s^k \tag{3.1}$$

$$\underline{\psi}_s^k = (L_m + L_{\sigma s})\,\underline{i}_s^k + L_m\left(\underline{i}_{r1}^k + \underline{i}_{r2}^k + \underline{i}_{r3}^k\right) \tag{3.2}$$

The electromagnetic torque is calculated by

$$T_e = \frac{3}{2} p \mathrm{Im}\left\{\underline{\psi}_s^{k*}\underline{i}_s^k\right\} \tag{3.3}$$

The circuit model was built in Matlab Simulink from the voltage and flux equations as shown in Figure 3.8. The stator voltages, currents and speed ω_r are measured from an operating motor or obtained by time-stepping FEA. The voltage is supplied to the circuit model in the time domain via Matlab Simulink. As shown in Figure 3.8, the parameters were estimated by minimizing the error I between the current response of the circuit i_{est} and the stator current in the transient or steady states.

The estimated parameters were used to calculate the electromagnetic torque by (3.3). Figure 3.9 shows a comparison of the torque responses in

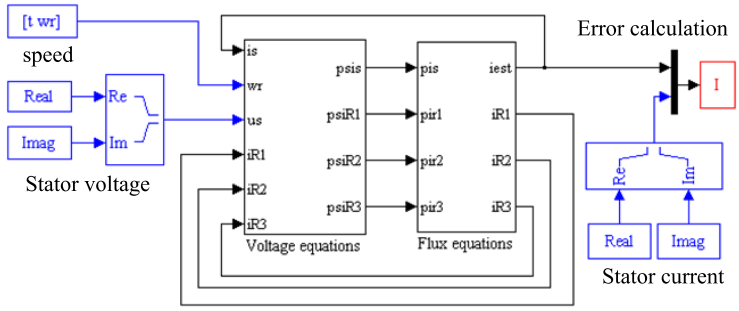

Figure 3.8. Electrical circuit model.

the transient stage when the motor is being supplied by a rated voltage. The torque calculated by the constant parameters of the circuit T_{e} well tracks the torque calculated by the time-stepping FEA T_{FEA}. Therefore, an appropriate circuit with constant parameters may predict the electromagnetic torque in the transient state.

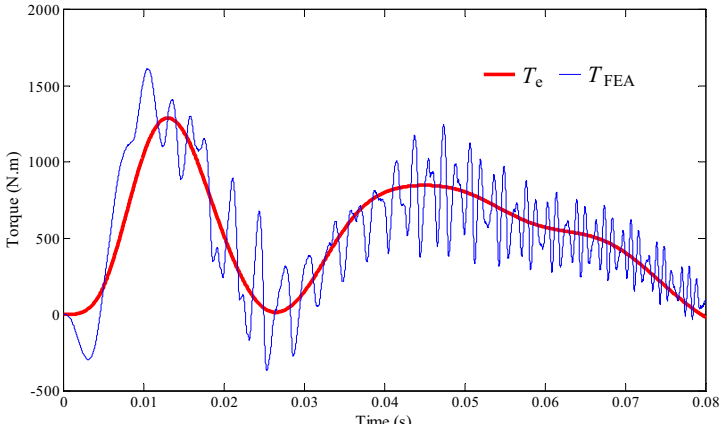

Figure 3.9. Torque response during estimated period.

In addition, the stator and rotor resistive losses can be calculated from the rms value of the currents (capital letters) and resistances in the circuit branches as follows.

$$P_{\mathrm{st}} = \frac{3}{2} R_{\mathrm{s}} I_{\mathrm{s}}^2 \tag{3.4}$$

$$P_{\mathrm{rt}} = \frac{3}{2} \left(R_{\mathrm{r1}} I_{\mathrm{r1}}^2 + R_{\mathrm{r2}} I_{\mathrm{r2}}^2 + R_{\mathrm{r3}} I_{\mathrm{r3}}^2 + R_{\mathrm{c2}} I_{\mathrm{r12}}^2 + R_{\mathrm{c1}} I_{\mathrm{r}}^2 \right) \tag{3.5}$$

where

$\underline{i}_{\mathrm{r}} = \underline{i}_{\mathrm{r1}} + \underline{i}_{\mathrm{r2}} + \underline{i}_{\mathrm{r3}}$

$\underline{i}_{\mathrm{r12}} = \underline{i}_{\mathrm{r1}} + \underline{i}_{\mathrm{r2}}$

The resistive losses of a 37-kW induction motor can be predicted from the circuit when the parameters of the circuit are accurately identified. The resistive losses were calculated from the constant resistances and rms currents in the circuit branches as in (3.4) and (3.5). Figures 3.10 and 3.11 show the resistive losses calculated by the circuit (dots) and FEA (solid-blue lines) when the number of data points in a period used for the estimation is increased.

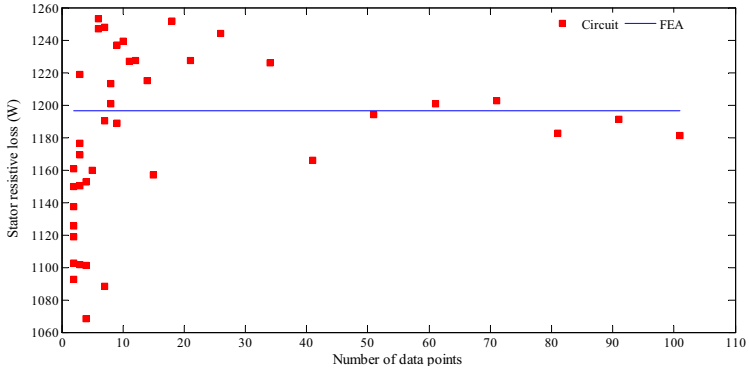

Figure 3.10. Stator resistive loss of a 37 kW induction motor.

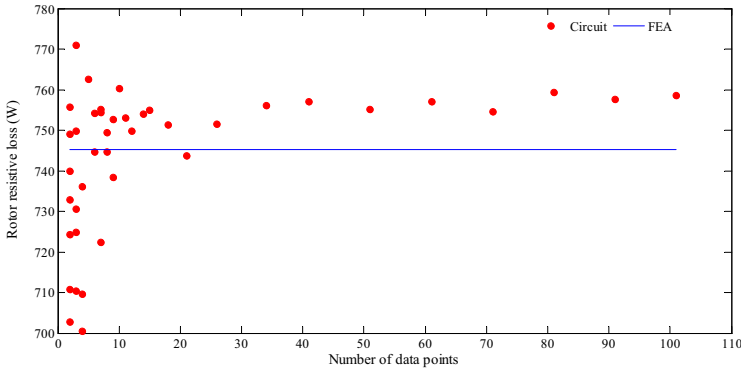

Figure 3.11. Rotor resistive loss a 37 kW induction motor.

More details and discussion of the loss calculation and estimation method in the time domain can be found in Publication III.

3.2.2 Resistive loss modelling for a high-power induction motor

As shown in Figure 3.1, the resistive-loss distribution in the stator bars of a 1250-kW motor indicates that using a sole dc resistance cannot model the eddy-current losses of the stator windings. The current or loss density is not homogeneous over the cross-section of the stator slot. A similar phe-

nomenon also occurs in semi-open rotor slots (Publication IV). When the T-equivalent circuit shown in Figure 3.12 represents the 1250-kW form-wound IM, the transfer function of the small-signal impedance of the motor in the stator reference frame can be written as in (3.6) as $s = j\omega$. Details of the impulse method and small-signal models can be found in Repo (2008).

$$\underline{Z}_{\mathrm{e}} = \frac{\underline{Z}_{\mathrm{s}}\left(\underline{Z}_{\mathrm{m}} + \underline{Z}_{\mathrm{r}}\right) + \underline{Z}_{\mathrm{m}}^{'} Z_{\mathrm{r}}}{\underline{Z}_{\mathrm{m}} + \underline{Z}_{\mathrm{r}}} = \frac{\Delta \underline{u}_{\mathrm{s}}}{\Delta \underline{i}_{\mathrm{s}}} \tag{3.6}$$

where

$$\underline{Z}_{\mathrm{s}} = R_{\mathrm{s}} + sL_{\sigma\mathrm{s}} \tag{3.7}$$

$$\underline{Z}_{m} = sL_{\mathrm{m}} - j\omega_0 L_{\mathrm{m}} \tag{3.8}$$

$$\underline{Z}_{m}^{'} = sL_{\mathrm{m}} \tag{3.9}$$

$$\underline{Z}_{\mathrm{r}} = R_{\mathrm{r}} + sL_{\sigma\mathrm{r}} - j\omega_0 L_{\sigma\mathrm{r}} \tag{3.10}$$

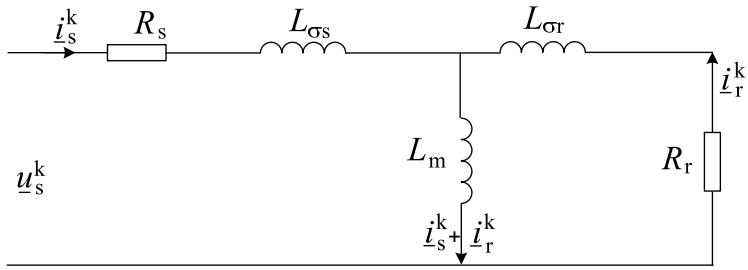

Figure 3.12. T - equivalent circuit.

The frequency response of the circuit is quite different from that of the motor as shown in Figure 3.13. In the figure, Z_{m} is the FRF obtained from the impulse method and the Z_{e} is the FRF from the circuit model. The imaginary and real parts are marked *i* and *r* in the figure.

The Cauer ladder circuit was used to model the skin effect or eddy currents in the motor (Krah 2005). The equivalent circuit for the form-wound IM is presented in Figure 3.14. The mathematical meaning of the extra Cauer ladders is that they increase the order of the impedance FRF and add degrees of freedom. As shown in (3.11) and (3.12), the orders of stator and rotor impedances were increased, so they increase the order of the total impedance (3.6).

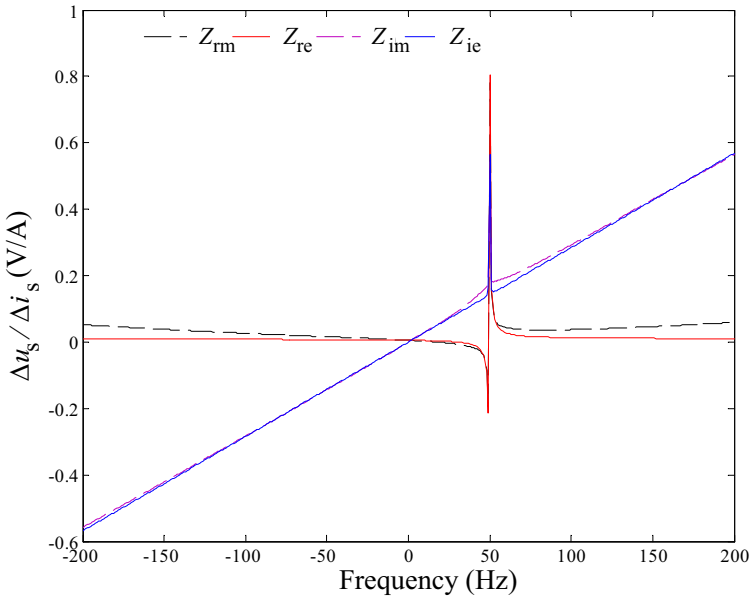

Figure 3.13. Frequency response of T - circuit model.

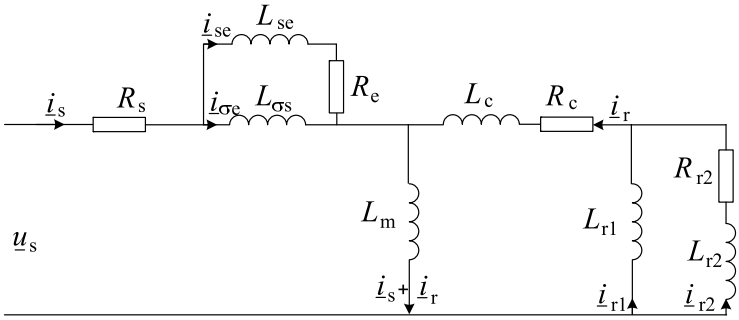

Figure 3.14. Equivalent circuit for the form-wound IM.

$$\underline{Z}_{\mathrm{s}}(s) = R_{\mathrm{s}} + \frac{sL_{\sigma\mathrm{s}}(R_{\mathrm{e}} + sL_{\mathrm{se}})}{sL_{\sigma\mathrm{s}} + R_{\mathrm{e}} + sL_{\mathrm{se}}} \tag{3.11}$$

$$\underline{Z}_{\mathrm{r}}(s) = R_{\mathrm{c}} + (s - j\omega_0)\, L_{\mathrm{c}} + \underline{Z}_{\mathrm{r12}} \tag{3.12}$$

where

$$\underline{Z}_{\mathrm{r12}} = \frac{((s - j\omega_0)\, L_{\mathrm{r1}})(R_{\mathrm{r2}} + (s - j\omega_0)\, L_{\mathrm{r2}})}{(s - j\omega_0)\, L_{\mathrm{r1}} + R_{\mathrm{r2}} + (s - j\omega_0)\, L_{\mathrm{r2}}} \tag{3.13}$$

$$\underline{\psi}_{\mathrm{s}} = L_{\sigma\mathrm{s}}\underline{i}_{\sigma\mathrm{s}} + L_{\mathrm{se}}\underline{i}_{\mathrm{se}} + L_{\mathrm{m}}(\underline{i}_{\mathrm{r1}} + \underline{i}_{\mathrm{r2}} + \underline{i}_{\sigma\mathrm{s}} + \underline{i}_{\mathrm{se}}) \tag{3.14}$$

The impedance FRF of the circuit fits well to the data from FEA simulation as shown in Figure 3.15. When the motor is fed by a frequency converter, the supply voltage is highly distorted by harmonics. The control algorithm of the converter needs a circuit model, which is valid over a wide range of frequencies. The proposed circuit model is valid from -200 Hz to 200 Hz, and has constant parameters. The difficulty of the fitting lies in the frequency range 0-100 Hz in Figure 3.15, so the frequency range of the circuit can be easily expanded to higher frequencies than 200 Hz. Therefore, not only does the model represent the motor well, but it is also simple to implement in the motor control.

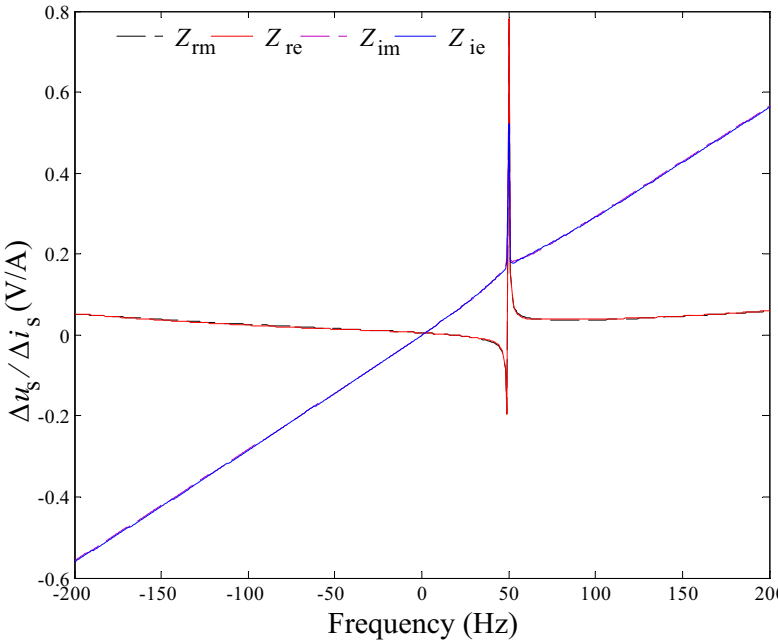

Figure 3.15. Frequency response of the proposed model.

The total resistive loss of the motor is calculated as

$$P_t = \frac{3}{2}\left(R_\mathrm{s} I_\mathrm{s}^2 + R_\mathrm{e} I_\mathrm{e}^2 + R_\mathrm{c} I_r^2 + R_\mathrm{r2} I_\mathrm{r2}^2\right) \tag{3.15}$$

The parameters of the circuit were used to predict the resistive losses and the torque of the motor. The deviation between the predicted performance by using the circuit and FEA is less than 3%. Details of the research can be found in Publication IV.

3.3 Temperature rise analysis

The electromagnetic losses cause a temperature rise in electrical machines, so the temperature rise analysis is the next step in the study of the resistive loss modelling. The thermal analysis of electrical machines using random-wound windings can be found in the reports reviewed in the literature (Boglietti et al. 2009a). In this section, the temperature rise analysis for induction motors using form-wound windings will be presented for two methods: FEA and thermal networks.

3.3.1 Temperature rise analysis using FEMM

To know how the inhomogeneous losses lead to a temperature distribution in the stator slot of a 1250-kW form-wound IM, the public domain code FEMM was used to analyze the temperature rise. The heat conduction of the conductor bars obeys Gauss's law in (3.16). The convection boundary of insulation inside air or slot-wedge inside air is described by (3.17). Figure 3.16 shows that the hottest spot is the bar closest to the air-gap. This leads to a big difference between the maximum temperature and average temperature within the stator slot. However, the IEC 60034-1 standard proposes that the difference should be smaller than 10 K in a good electrical machine (IEC 60034-1 2004). The radial position of the conductor should be adjusted to conform to the IEC standard.

$$-\nabla \cdot (\lambda \nabla T) = p_{\text{loss}} \tag{3.16}$$

$$\lambda \frac{\partial T}{\partial n} + h\,(T - T_0) = 0 \tag{3.17}$$

As shown in Section 3.1, the magnetic slot wedges help to reduce the eddy-current losses of the induction motor. The temperature rise analyses of the stator with and without the use of magnetic slot wedges are shown in Figure 3.17. As shown in Publication II, the radial position has to be larger than 5.8 mm for the stator without the magnetic slot wedges. If the magnetic slot wedges are used, this distance can be reduced to 4.8 mm, or the machine diameter reduced by 2 mm. Anyway, the reduction of the eddy-current losses as a result of using the magnetic slot wedges reduces the outer diameter of the stator core or motor volume. The details can be found in Publication II.

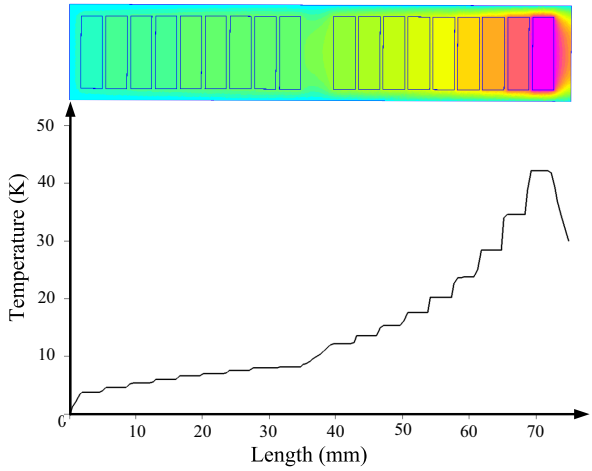

Figure 3.16. Temperature-rise distribution in the stator slot.

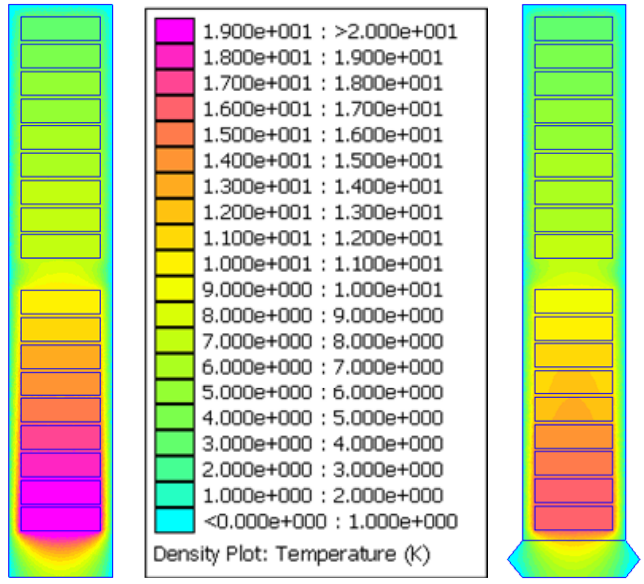

(a) without wedge (b) with wedge

Figure 3.17. Temperature-rise in the stator slot with and without slot wedge.

3.3.2 Temperature rise analysis using thermal networks

For a faster temperature rise analysis, thermal networks were widely used for years (Demetriades et al. 2010, Howey et al. 2012). For high-speed machines, a thermal network model was developed and validated by Saari (1998). The model was used to analyze the temperature rise of an HSIM using random-wound stator windings. The equivalent thermal resistances in the stator and definition of thermal directions are shown in Figure 3.18. Within a stator slot, the equivalent thermal resistances of the random-wound winding are shown in Figure 3.19. In the stator slot, three resistances exist: slot contact (blue line), slot insulation (b_{ss}) and coils (inside). To apply the model to the HSIM using form-wound stator windings in Section 3.1, the thermal conductivities and resistances have to be redefined in this section. For the random-wound windings, the average thermal conductivities (coils or white background region in Figure 3.19) of the random-wound winding in the circumferential and radial directions are equal (Pyrhönen et al. 2009).

$$\lambda_{\mathrm{av-cr}} \approx \lambda_{\mathrm{i}} \left(\frac{D_{\mathrm{c}}}{D - D_{\mathrm{c}}} + \frac{D - D_{\mathrm{c}}}{D} \right) \tag{3.18}$$

The thermal conductivity of copper λ_{w} is thousands of times higher than that of the insulation λ_{i} . It is reasonable to assume that the thermal resistance of copper is zero when calculating the average thermal conductivity $\lambda_{\mathrm{av-cr}}$ of the random-wound windings. In the calculation of the average thermal conductivity, the thermal conductivity of the insulation, 0.15 W/(m·K), is quite small when compared to the thermal conductivity of copper, 333 W/(m·K). Consequently, the circumferential or radial thermal conductivity is 0.866 W/(m·K) in the coil region.

When the same approach is applied to form-wound stator windings in the Publication V, the average thermal conductivities of the coil or copper bar region are re-defined because they are different in the circumferential and radial directions. The circumferential thermal conductivity is applied for the core region, while the radial thermal conductivity is used in the calculations for the end-winding. Figure 3.20 shows a principle to calculate the thermal conductivities in those directions.

The circumferential thermal conductivity of a form-wound stator slot is calculated by (3.19) referred to in Figure 3.20 (b). In this direction, the copper bar is directly involved in thermal conduction. There are no in-

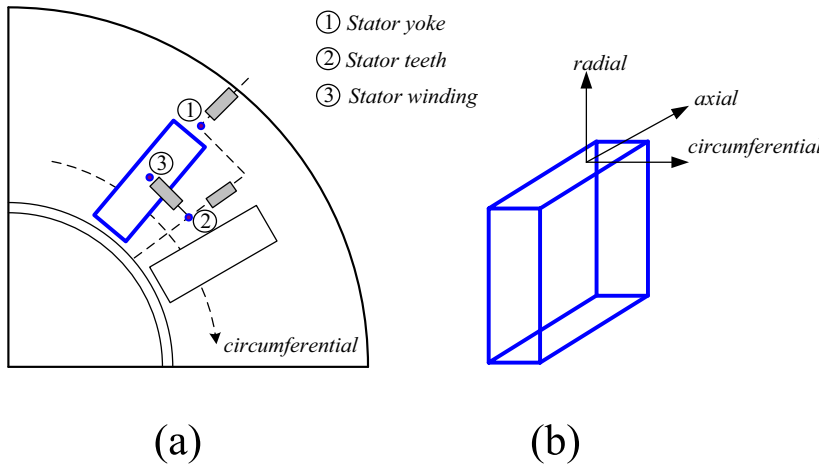

Figure 3.18. Connection of thermal resistances in the stator core (a) and definition of directions (b).

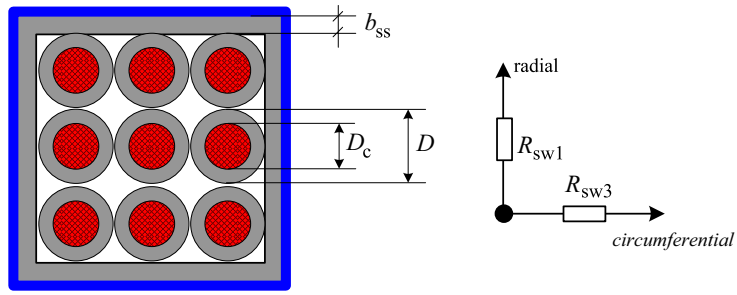

Figure 3.19. Random-wound winding and its equivalent thermal resistances.

sulation layers with a low conductivity in the circumferential direction of the copper height 12 h_c or 18 mm while the insulation height is about 10 mm. As a result, the average thermal conductivity in the circumferential direction of the form-wound winding of 198.2 W/(m·K) is significantly larger than that of the random-wound winding of 0.866 W/(m·K).

$$\lambda_{av-c} = \frac{\lambda_i h_{is} + \lambda_w 12 h_c}{h_{is} + 12 h_c} \tag{3.19}$$

where $h_{is} = H_1 - 12h_c$

The average thermal conductivity of a bar in the radial direction as shown in Figure. 3.20 (c) is calculated as

$$\lambda_{br} = \frac{2\lambda_i w_{ib} + \lambda_w \left(B_{12} - 2w_{is} - 2w_{ib}\right)}{B_{12} - 2w_{is}} \tag{3.20}$$

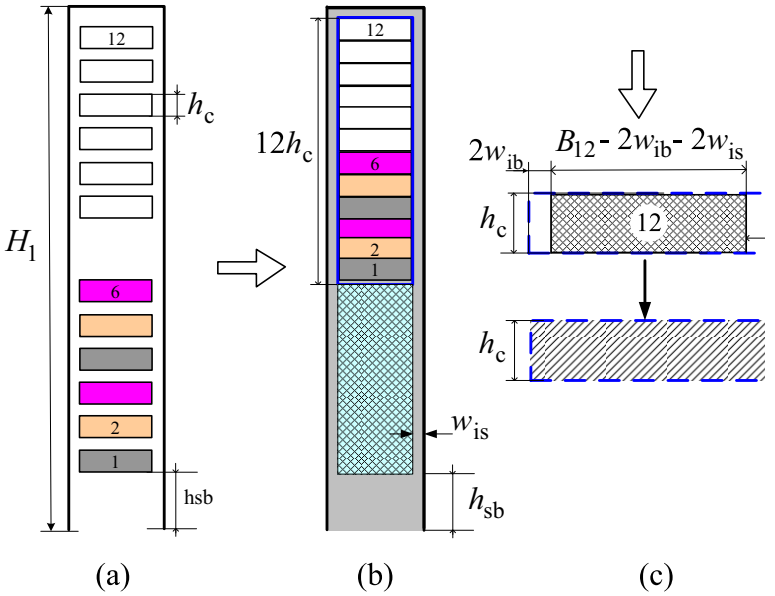

Figure 3.20. Form-wound winding stator slot (a), equivalent model for calculating circumferential (b) and radial (c) thermal conductivities.

Radial thermal conductivity for the stator slot of 12 copper bars is

$$\lambda_{\mathrm{sr}} = \frac{\lambda_{\mathrm{br}}\lambda_{\mathrm{i}}}{12h_{\mathrm{c}}\lambda_{\mathrm{i}} + (H_1 - 12h_{\mathrm{c}} - h_{\mathrm{sb}})\,\lambda_{\mathrm{br}}} \tag{3.21}$$

In the radial direction, the conduction surface of the form-wound winding is higher than that of the random-wound winding. This also leads to a higher average thermal conductivity of the form-wound winding of 12.75 W/(m·K) as compared to the 0.866 W/(m·K) of the random-wound winding in the radial direction.

In the end-winding region, the heat transfer includes conduction and convection. Heat-transfer coefficients were already defined in Saari (1998) where the structure of the end-winding of the motor using random-wound windings was shown in Figure 3.21. When the model for the HSIM using the form-wound stator windings is being applied, the cooling area of the end-winding should be clarified. The end-winding model of the 300-kW HSIM assumed in Figure 3.5 of Section 3.1 is shown in Figure 3.22. From this model, both the thermal conduction and convection resistances were calculated. For instance, the axial conduction resistance R_{ew1} and radial conduction resistance R_{ew2} were calculated from the dimensions of the end-winding by using the winding conductivity λ_{w} and radial conductivity λ_{sr} as follows

$$R_{\mathrm{ew1}} = \frac{l_{\mathrm{end}} + \frac{l_{\mathrm{a-end}}}{2}}{N_1 N_{\mathrm{s}} \pi h_{\mathrm{c}} w_{\mathrm{c}} \lambda_{\mathrm{w}}} \tag{3.22}$$

$$R_{\mathrm{ew2}} = \frac{ln\left(\frac{D_{\mathrm{wo}}}{D_{12}+h_{\mathrm{sb}}}\right)}{2\pi l_{\mathrm{a-end}} \lambda_{\mathrm{rw}}} \tag{3.23}$$

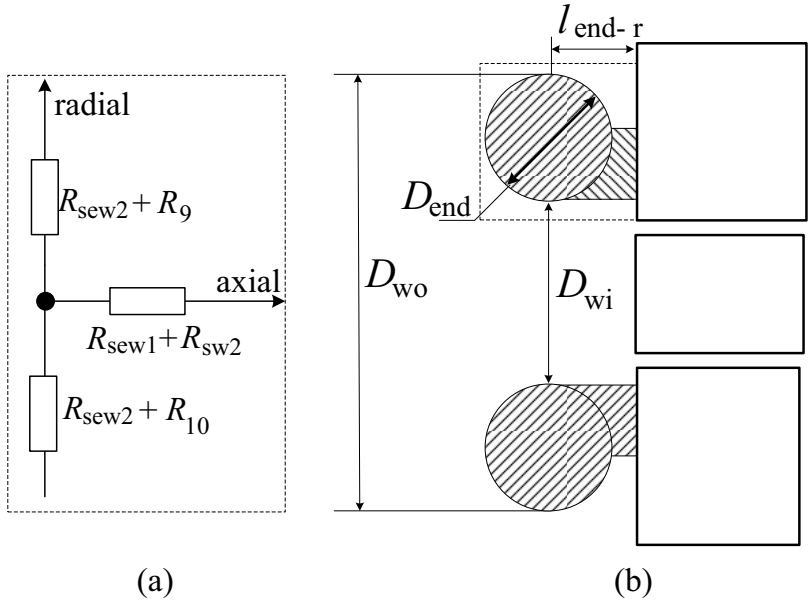

Figure 3.21. End-winding model for the random-wound stator winding.

The equations to calculate the convection thermal resistances R_9 and R_{10} of the thermal network and convection heat-transfer coefficients in Saari (1998) are re-used, but the cooling end-winding area is calculated on the basis of Figure 3.22:

$$A_{\mathrm{ew1}} = 2\pi(3w_{\mathrm{c}} + D_{\mathrm{wo}} - D_{12} - h_{\mathrm{sb}})D_{\mathrm{wo}} \tag{3.24}$$

It can be seen from the literature (Mesrobian and Holdrege 1990), Section 3.1, and the analysis of thermal conductivities that high thermal conductivity, robust structure and high reliability are typical advantages of form-wound windings. The performance of the form-wound stator winding for a HSIM can be further studied numerically by means of the loss minimum design, as introduced in the next section.

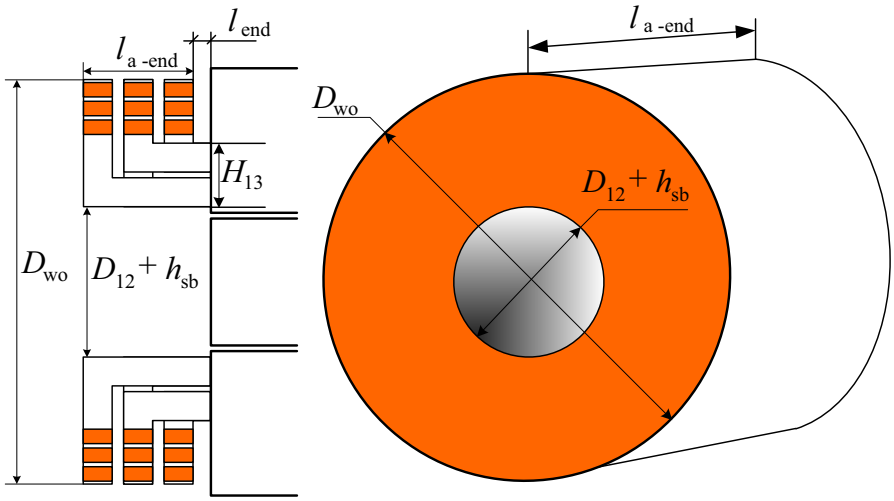

Figure 3.22. End-winding model for the form -wound stator winding.

3.4 Resistive loss minimization for form-wound stator windings

The main purpose of modelling losses in electrical machines is to collect sufficient information on the losses and to reduce the losses in the machines. The resistive loss in the random-wound winding is quite challenging to model. This may cause inaccuracy in the optimal design of the motor. In the previous sections, the tools that can be used to model resistive losses and temperature rises in form-wound stator windings were presented. This section presents a procedure to reduce those losses in HSIMs under the constraints of temperature rise and insulation thickness. As an example, Figure 3.23 shows a form-wound stator winding of a 300-kW HSIM and related dimensions. The main objective is to minimize the resistive losses in the stator windings of the motor.

As mentioned in Publication V, time-discretized FEA is used to model the ac stator resistive loss (dc and eddy-current loss) in the stator winding. To maintain the accuracy of the eddy-current modelling, finite-element meshes are sufficiently detailed to model eddy-current effects in a stator winding supplied by PAM voltages. Each conductor is always subdivided into two layers with 8 second-order finite elements. The flux distribution of a roughly-designed motor, presented in Section 3.1, is shown in Figure 3.24, which is of the motor before the optimization. The calculated electromagnetic losses from time-discretized FEA serve as the input for

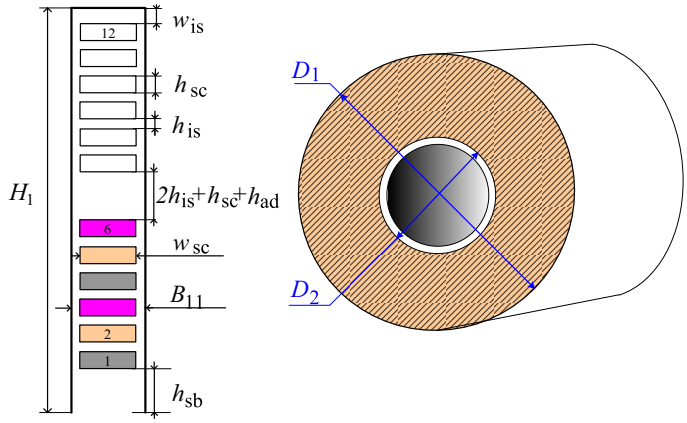

Figure 3.23. Stator slot model and motor model.

the temperature rise analysis to check the temperature rise constraints (Saari 1998).

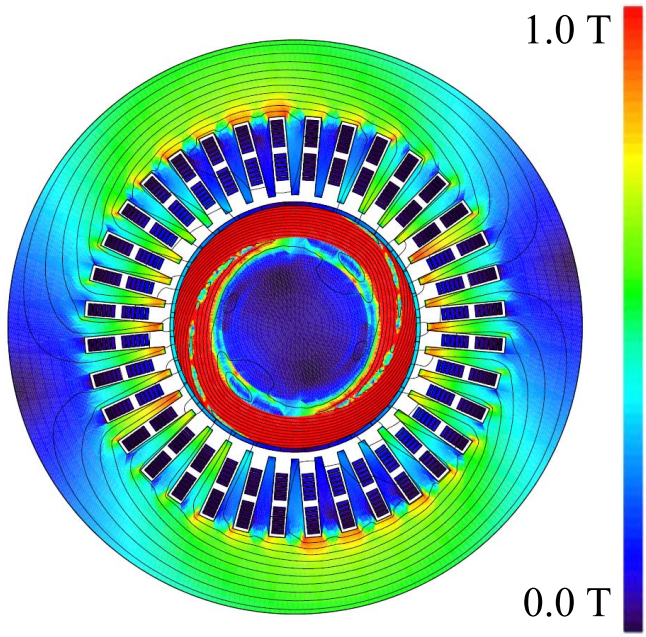

Figure 3.24. Flux distribution of HSIM before the optimization.

A flow chart to reduce the electromagnetic losses of electrical machines is presented in Figure 3.25. Publication V applies this flow chart to minimize the resistive losses in the stator form-wound winding of the HSIM. To reduce the time consumption of a design, the Taguchi approach was used to study which parameters are important for the design problem (Hwang et al. 2012). The height of the conductor h_{sc} and the distance from

the top bar to the air-gap h_{sb} are the two most important parameters for minimizing the resistive loss as shown in Figure 3.26, while the influence of the width of the slot B_{11} and the inner diameter of the stator D_2 is quite small. As a result of the evaluation, some insignificant parameters were eliminated from the optimization. Therefore, the computational cost of the design problem was significantly reduced.

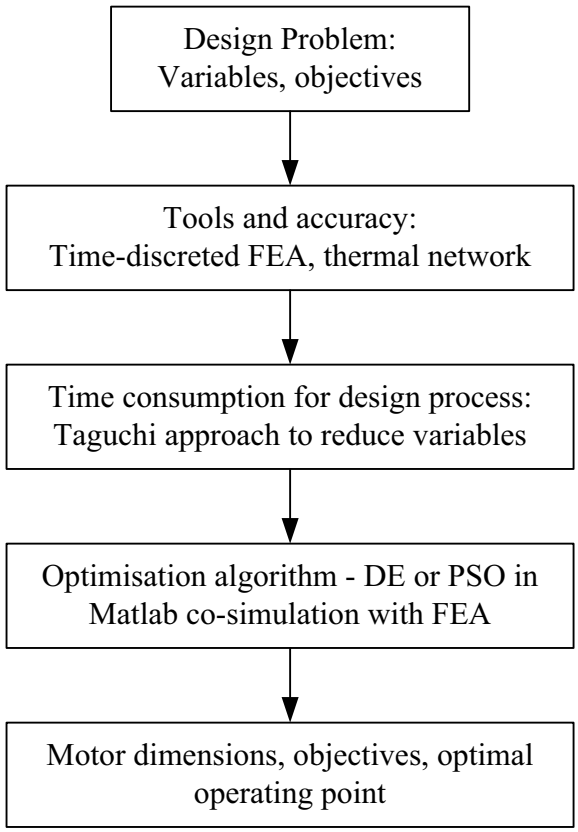

Figure 3.25. A procedure to minimize electromagnetic losses in the stator form-wound winding.

In the design problem, the height of the conductor h_{sc} and the distance from the top bar to the air gap h_{sb} are dependent variables. Within a stator slot, an increase in the height of the conductor h_{sc} leads to a decrease of h_{sb}. An optimization is required to deal with this conflict. There are many popular optimizations that are used in the machine designs, such as particle swarm optimization (PSO), genetic algorithm (GA) or differential evolution (DE), etc (Lee and El-Sharkawi 2008). In this study, DE was selected to minimize the resistive losses in the form-wound stator windings of the HSIM.

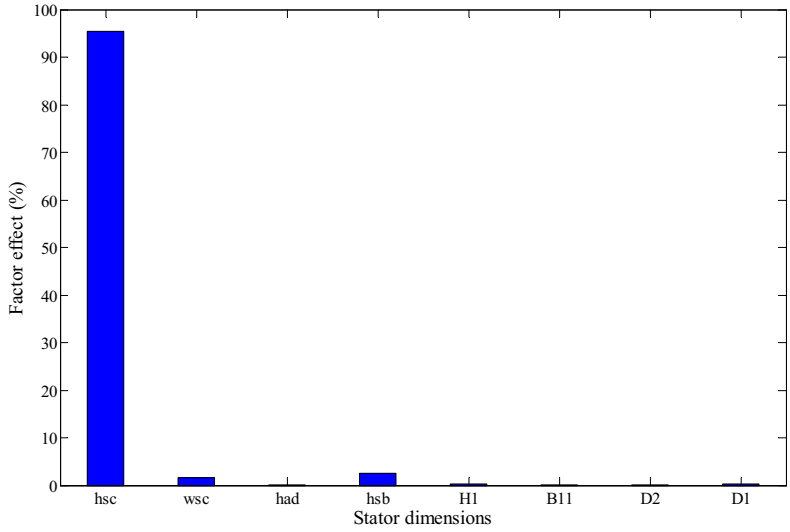

Figure 3.26. Factor Effect of stator dimensions on stator resistive loss.

In the design process of HSIMs, it is necessary to check the temperature rise, power factor, and insulation constraints. The temperature rise was analyzed by using the thermal network described in Section 3.3.2. The optimization and thermal analysis were built in Matlab. As a result, a Matlab co-simulation with time-stepping FEA was proposed in the design process as shown in Figure 3.27 (Publication V). The importance of having sufficient information was emphasized by the optimization with sinusoidal and PAM supplies. In all the cases, the motor was run at a constant slip of 1 %.

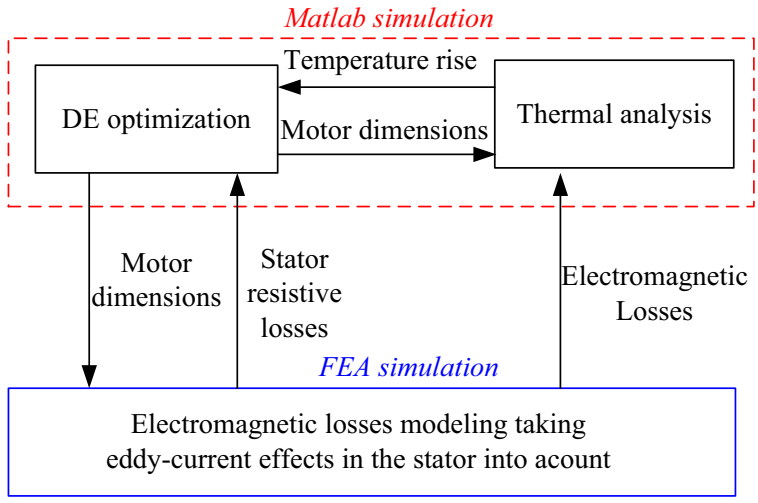

Figure 3.27. Co-simulation model.

Table 3.2. Initial and optimal dimensions.

	initial	Optimal - sin	Optimal- PAM
h_{sc} (mm)	1.5	1.58	1.30
w_{sc} (mm)	5.0	5.80	5.80
h_{sb} (mm)	3.0	9.88	10.0
H_1 (mm)	34.25	39.4	40.0
D_1 (mm)	250	260.8	283
Filling factor	0.375	0.3976	0.323

Table 3.3. Initial and optimal performance.

	i-sin	op-sin	i-PAM	op-PAM
Stator dc resistive loss (W)	2732.4	2178.0	2808.5	2824.1
Stator ac resistive loss (W)	3384.7	3020.4	4286.0	3825.6
Core region (W)	1426.2	1459.4	2273.0	1801.2
End-winding (W)	1958.4	1561.0	2012.9	2024.4
Stator core loss (W)	947.2	996.6	946.4	854.9
Rotor resistive loss (W)	3132.5	3029.3	4146.5	3993.3
Rotor core loss (W)	781.4	771.1	1310.7	1237.3
Total loss (W)	8871.9	8420.6	10692.2	9913.6

i-sin = initial-sin, op-sin= optimal-sin

i-PAM = initial PAM, op-PAM= optimal PAM

With PAM supply, the electromagnetic torque during the optimization varied insignificantly around the value of 45.3 Nm and was assumed to be a constant throughout the process. Table 3.2 shows the initial dimensions and optimal dimensions using the sinusoidal and PAM supplies. The optimization using the sinusoidal supply reduces the dc resistive losses as shown in Table 3.3 or increases the copper area or filling factor as shown in Table 3.2. However, when the motor is supplied with the PAM voltage, the optimization tries to reduce the eddy-current losses in the stator slots, while the dc resistive loss remains more or less the same. The reduction of the ac stator resistive loss by about 10 % allows the machine to be much cooler on the stator side as shown in Table 3.4. The power factor of the machine is about 0.75, and the maximum torque defined from the characteristic curve (torque versus speed) is 85.5 Nm.

Table 3.4. Temperature rise with PAM supply.

	initial	optimal
Average stator winding (°C)	145.9	124.3
Stator winding in core (°C)	154.9	118.4
Stator winding in end-region (°C)	141.4	128.8
Rotor coating (°C)	134.8	130.6
Rotor end-ring(°C)	134.6	130.4

Details of the study can be found in Publication V.

4. Discussion and conclusions

This chapter first summarizes the research work and discusses possible study in the future. Then conclusions after the work are given at the end.

4.1 Summary and significance of the research

To investigate the possibility of using one equivalent circuit for predicting the resistive losses in the induction motors, higher harmonics are superimposed on the fundamental voltage. This is performed by means of FE simulations. It is discovered that the resistive losses are dependent on the harmonic amplitudes and independent of the harmonic phases. It seems that an appropriate circuit representing the motor is sufficient to predict the resistive losses, including higher harmonics.

In Repo (2008), it was shown that a triple-cage circuit can model the eddy-currents of a deep-bar induction motor. The circuit parameters were estimated in steady state by time-harmonic FEA, which requires the motor information, typically motor materials and structure. Unfortunately, the estimation using FEA may have negative parameters with nonphysical meaning. To overcome those problems, a method to estimate the parameters of the triple-cage circuit in the time domain is proposed by using differential evolution. When the parameters of the circuit are accurately estimated, the triple-cage circuit predicts the motor performance well in both the steady and transient states.

From the FE modelling developed by Jahirul Islam (2010), it was found that the eddy-current effects in a form-wound induction motor cannot be neglected in the design stage. In this study, by using that FE model to collect the resistive losses for a temperature rise analysis using FEMM, it is shown that the hottest spot in the form-wound stator is the bar closest to the air-gap. To have a good design for the form-wound winding of a

high-power motor, as proposed in the IEC-standard (IEC 60034-1 2004), the stator bars should be fitted far away from the air-gap. Slot wedges can reduce the resistive losses in the stator and indirectly reduce the volume of the machine as well.

A traditional T-equivalent circuit representing an induction motor implies that the resistive-loss distribution in the stator is homogeneous and the stator winding can be represented by a sole dc resistance. However, when the eddy-current effect is significant, an advanced circuit model is needed. An equivalent circuit that is suitable for modelling a form-wound induction motor is presented in this research. The eddy-current losses can be taken into account by adding extra circuit branches to the T-equivalent circuit. The parameters are estimated over a wide range of frequencies for applications in electric drives.

In the design process of electrical machines, technological constraints such as temperature rises, insulation, etc. always have to be checked. This information is defined by specific numbers and calculated using different softwares. A co-simulation model was shown to provide a good solution for dealing with a design task that requires electromagnetic and thermal calculations and insulation constraints in an optimization . The time consumption of the optimization can be reduced by eliminating the unimportant variables of the problem by using the Taguchi approach.

It can be seen that, in order to minimize resistive losses in form-wound windings, information on the voltage supply is very important. Depending on the voltage supply, the optimization increases or reduces the conductor height or copper area to reach a minimum loss. If the machine is assumed to be operating at a sinusoidal supply at the design stage, it is not necessarily optimized from the perspective of losses at a PAM supply, and vice versa.

4.2 Discussion of the work

A study of the effect of a PWM supply on the resistive losses was implemented by FEA. A validation of the study by experimental results was lacking. In an inverter-fed motor, the PWM supply involves many higher harmonics, but this study considers the effect of individual higher harmonics.

In this study, time-discretized FEA was used to accurately model the electromagnetic losses in electrical machines. The temperature rise re-

sulting the losses was analyzed in order to adjust the design of form-wound stator windings as proposed by IEC 60034-1 (2004). This work focuses on taking into account eddy-current losses in stator conductors and their effect on the temperature rise. Other electromagnetic losses were modelled by traditional FEA methods. The method for modelling the eddy-current losses was not further developed beyond the work of Jahirul Islam (2010). In order to overcome the drawbacks of the method, such as the requirement of a detailed mesh, the model should be additionally improved.

A method to estimate the parameters of a triple-cage circuit in the time domain was presented. The method identifies the parameters at certain operating points. As a result of this research, fundamental components of resistive losses and electromagnetic torque and the torque response in the transient stateare predicted by using the circuit model. No model that took saturation and the effect of slot harmonics into account was introduced in the study. The estimation method was separately applied in the transient and steady states. The combination of the parameters between those states has not been studied yet.

An equivalent circuit representing a form-wound induction machine was introduced. The parameters of the circuit were estimated in the frequency domain by an impulse method (Repo 2008). The measurement of impulse signals is still very challenging in a real setup. A method to estimate the circuit parameters based on measured signals, typically fundamental stator currents and voltages, needs to be developed.

The temperature rise in electrical machines resulting from electromagnetic loss was analyzed by FEA and an analytical model. For the FEA approach, thermal modelling using FEMM is a very simple way of checking the temperature difference among the conductors in a stator slot. The thermal model is for a sole slot, so the interaction between stator slots and other parts of the motor is lacking. The thermal exchange among components should be comprehensively considered for a better evaluation of the temperature rise of electrical machines. Within the analytical approach, the thermal analysis involved whole components of machines by using a thermal network developed by Saari (1998). The challenge of defining heat-transfer coefficients was solved in that report. To apply the model for a thermal analysis of the motor using form-wound stator windings, the structure of the stator windings and thermal conductivities were redefined in this study. However, the structure of a prototype may be dif-

ferent from the model that was designed. The air-space and cooling area were not well specified in the present research.

As a main purpose of loss modelling, loss minimization in the form-wound stator winding was obtained from a Matlab co-simulation with FEA. This work concentrated on resistive losses. However, many other loss components are involved in the design process of electrical machines. In order to find a design for which all the loss components are minimized, a multi-objective optimization for the machines is required (Di Barba 2010). Unfortunately, modelling for other electromagnetic losses is still a challenge in multi-objective optimization as a result of the lack of proper models. The selection of optimizations is always debated, so which optimization is best for the optimal design of electrical machines is not confirmed by this research.

4.3 Conclusions

The importance of modelling resistive losses in electrical machines was emphasized in this study. For high accuracy modelling, time-discretised FEA was used to simulate induction motors using form-wound stator windings. A co-simulation model to reduce or minimize resistive loss in the form-wound stator winding of a 300-kW high-speed induction motor was introduced. Within the design process, the type of voltage supply is very important information in the minimisation of the resistive loss. Prior to final loss minimization, variables in the optimization problem or time-computational cost can be reduced by using the Taguchi method.

Following IEC 60034-1 (2004), the resistive losses in the form-wound stator winding of a 1250-kW machine were reduced in order to have a good design from the temperature rise point of view. In this process, the temperature rise analysis can be simply implemented by the public code FEMM, while the resistive losses are modelled by time-discretised FEA.

To model resistive losses in electrical machines, circuit models were shown as a promising option. A single circuit can be used to predict the performance of the induction motors sufficiently. A time-domain optimization method to estimate the parameters of a triple-cage circuit was presented. The circuit parameters obtained were used to predict the performance of electrical machines. For modelling the eddy-current losses in a form-wound induction motor, an equivalent circuit was developed by adding extra branches to the T-equivalent circuit. The possibility of using

the circuit in electric drives was shown by the estimation of the circuit parameters through a range of frequencies.

References

Amara, Y., Reghem, P. and Barakat, G. (2010), 'Analytical prediction of eddy-current loss in armature windings of permanent magnet brushless ac machines', *IEEE Trans. Magn.* **46**(8), 3481–3484.

Arkkio, A. (1987), 'Analysis of Induction Motors Based on the Numerical Solution of the Magnetic Field and Circuit Equations', PhD thesis, Helsinki University of Technology, Espoo, Finland. http://lib.tkk.fi/Diss/198X/isbn951226076X/.

Bazzi, A. M. and Krein, P. T. (2010), 'Review of methods for real-time loss minimization in induction machines', *IEEE Trans. Ind. Appl.* **46**(6), 2319–2328.

Ben-Gal, I. (2005), 'On the use of data compression measures to analyze robust designs', *IEEE Trans. on Reliability* **54**(3), 381–388.

Boglietti, A., Cavagnino, A., Ferraris, L. and Lazzari, M. (2010), 'Impact of the supply voltage on the stray-load losses in induction motors', *IEEE Trans. Ind. Appl.* **46**(4), 1374–1380.

Boglietti, A., Cavagnino, A. and Lazzari, M. (2011), 'Computational algorithms for induction-motor equivalent circuit parameter determination - part I and II', *IEEE Trans. Ind. Electron.* **58**(9), 3723–3740.

Boglietti, A., Cavagnino, A., Staton, D., Popescu, M., Cossar, C. and McGilp, M. (2009b), 'End space heat transfer coefficient determination for different induction motor enclosure types', *IEEE Trans. Ind. Appl.* **45**(3), 929–937.

Boglietti, A., Cavagnino, A., Staton, D., Shanel, M., Mueller, M. and Mejuto, C. (2009a), 'Evolution and modern approaches for thermal analysis of electrical machines', *IEEE Trans. Ind. Electron.* **56**(3), 871–882.

Borisavljevic, A., Polinder, H. and Ferreira, J. (2010), 'On the speed limits of permanent-magnet machines', *IEEE Trans. Ind. Electron.* **57**(1), 220–227.

Bracikowski, N., Hecquet, M., Brochet, P. and Shirinskii, S. V. (2012), 'Multiphysics modeling of a permanent magnet synchronous machine by using lumped models', *IEEE Trans. Ind. Electron.* **59**(6), 2426–2437.

Briz, F., Degner, M. W. and Lorenz, R. D. (2000), 'Analysis and design of current regulators using complex vectors', *IEEE Trans. Ind. Appl.* **36**(3), 817–825.

Centner, M. and Schafer, U. (2010), 'Optimized design of high-speed induction motors in respect of the electrical steel grade', *IEEE Trans. Ind. Electron.* **57**(1), 288–295.

Demetriades, G., de la Parra, H., Andersson, E. and Olsson, H. (2010), 'A real-time thermal model of a permanent-magnet synchronous motor', *IEEE Trans. Power Electron.* **25**(2), 463–474.

Di Barba, P. (2010), 'Multiobjective shape design in electricity and magnetism', *Lecture Notes in Electrical Engineering, Springer* **47. ISBN 978-90-481-3079-5**.

Di Barba, P. (2011), 'Remarks on optimal design method in electromagnetics', *ICS Newsletter* **18**(2).

Dolinar, D., De Weerdt, R., Belmans, R. and Freeman, E. (1997), 'Calculation of two-axis induction motor model parameters using finite elements', *IEEE Trans. Energy Convers.* **12**(2), 133–142.

Faiz, J., Ganji, B., Carstensen, C., Kasper, K. and De Doncker, R. (2009), 'Temperature rise analysis of switched reluctance motors due to electromagnetic losses', *IEEE Trans. Magn.* **45**(7), 2927–2934.

Gao, X.-Z., Jokinen, T., Xiaolei, W., Ovaska, S. and Arkkio, A. (2010), A new harmony search method in optimal wind generator design, *in* 'Electrical Machines conference ICEM 2010'.

Gieras, J. and Saari, J. (2012), 'Performance calculation for a high speed olid-rotor induction motor', *IEEE Trans. Ind. Electron.* **59**(6), 2689–2700.

Gyselinck, J., Dular, P., Sadowski, N., Kuo-Peng, P. and Sabariego, R. (2010), 'Homogenization of form-wound windings in frequency and time domain finite-element modeling of electrical machines', *IEEE Trans. Magn.* **46**(8), 2852–855.

Hafiz, K., Nanda, G. and Kar, N. (2010), 'Performance analysis of aluminum- and copper-rotor induction generators considering skin and thermal effects', *IEEE Trans. Ind. Electron.* **57**(1), 181–192.

Harnefors, L. (2007), 'Modeling of three-phase dynamic systems using complex transfer functions and transfer matrices', *IEEE Trans. Ind. Electron.* **54**(4), 2239–2248.

Hettegger, M., Streibl, B., Biro, O. and Neudorfer, H. (2012), 'Measurements and simulations of the convective heat transfer coefficients on the end windings of an electrical machine', *IEEE Trans. Ind. Electron.* **59**(5), 2299–2308.

Hinkkanen, M., Repo, A.-K., Ranta, M. and Luomi, J. (2010), 'Small-signal modeling of mutual saturation in induction machines', *IEEE Trans. Ind. Appl.* **46**(3), 965–973.

Howey, D., Childs, P. and Holmes, A. (2012), 'Air-gap convection in rotating electrical machines', *IEEE Trans. Ind. Electron.* **59**(3), 1367–1375.

Huang, X., Goodman, A., Gerada, C. Y. F. and Lu, Q. (2012), 'Design of a five-phase brushless dc motor for a safety critical aerospace application', *IEEE Trans. Ind. Electron.* **59**(9), 3532–3541.

Huang, Y., Zhu, J. and Guo, Y. (2009), 'Thermal analysis of high-speed smc motor based on thermal network and 3-D FEA with rotational core loss included', *IEEE Trans. Magn.* **45**(10), 4680–4683.

Hwang, C. C., Li, P. L. and Liu, C. T. (2012), 'Optimal design of a permanent magnet linear synchronous motor with low cogging force', *IEEE Trans. Magn.* **48**(2), 1039–1042.

Hwang, S. H., Kim, J. M., Khang, H. V. and Ahn, J. W. (2010), 'Parameter identification of a synchronous reluctance motor by using a synchronous PI current regulator at a standstill', *J. Power Electron.* **10**(5), 491–497.

IEC 60034-1 (2004), *Rotating electrical machines, Machines Part I - Rating and Performance*, IEC 60034-1.

Inamura, S., Sakai, T. and Sawa, K. (2003), 'A temperature rise analysis of switched reluctance motor due to the core and copper loss by FEM', *IEEE Trans. Magn.* **39**(3), 1554–1557.

Islam, M., Islam, R., Sebastian, T., Chandy, A. and Ozsoylu, S. (2011), 'Cogging torque minimization in PM motors using robust design approach', *IEEE Trans. Ind. Appl.* **47**(4), 1661–1669.

Jahirul Islam, M. (2010), 'Finite-Element Analysis of Eddy Currents in the Form-wound Multi-conductor Windings of Electrical Machines', PhD thesis, Aalto University School of Science and Technology, Espoo, Finland. http://lib.tkk.fi/Diss/2010/isbn9789522482556/.

Jahirul Islam, M. and Arkkio, A. (2009), 'Effects of pulse-width-modulated supply voltage on eddy currents in the form-wound stator winding of a cage induction motor', *IET Electr. Power Appl.* **3**(1), 50–58.

Jahirul Islam, M., Pippuri, J., Perho, J. and Arkkio, A. (2007), 'Time-harmonic finite-element analysis of eddy currents in the form-wound stator winding of a cage induction motor', *IET Electr. Power Appl.* **1**(5), 839–846.

Jankowski, T., Prenger, F., Hill, D., O'Bryan, S., Sheth, K., Brookbank, E., Hunt, D. and Orrego, Y. (2010), 'Development and validation of a thermal model for electric induction motors', *IEEE Trans. Ind. Electron.* **57**(12), 4043–4054.

Kim, K., Lee, J., Kim, H. and Koo, D. (2009), 'Multiobjective optimal design for interior permanent magnet synchronous motor', *IEEE Trans. Magn.* **45**(3), 1780–1783.

Kolondzovski, Z., Arkkio, A., Larjola, J. and Sallinen, P. (2011), 'Power limits of high-speed permanent-magnet electrical machines for compressor applications', *IEEE Trans. Energy Convers.* **26**(1), 73–82.

Krah, J. H. (2005), 'Optimum discretization of a physical Cauer circuit', *IEEE Trans. Magn.* **41**(5), 1444–1447.

Lähteenmäki, J. (2002), 'Design and Voltage Supply of High-Speed Induction Machines', PhD thesis, Helsinki University of Technology, Espoo, Finland. http://lib.tkk.fi/Diss/2002/isbn951226224X/.

Laldin, O., Dlala, E. and Arkkio, A. (2011), 'Circuit models for predicting core losses in the stator and rotor of a caged induction machine with sinusoidal supplies', *IEEE Trans. Magn.* **47**(5), 1054–1057.

Lee, J., Kim, Y., Nam, H., Ha, K., Hong, J. and Hwang, D. (2004), 'Loss distribution of three-phase induction motor fed by pulsewidth-modulated inverter', *IEEE Trans. Magn.* **40**(2), 762–765.

Lee, K. and El-Sharkawi, M. (2008), *Modern heuristic optimization techniques - theory and application to power system*, John Wiley and Sons, Inc., Hoboken, New Jersey.

Li, W., Jeong, Y. W. and Koh, C.-S. (2010), 'An adaptive equivalent circuit modeling method for the eddy current-driven electromechanical system', *IEEE Trans. Magn.* **46**(6), 1859 – 1862.

Lin, R. (2010), 'Electromagnetic and Mechanical Finite Element Analysis of End Region of Large-Sized Three-Phase Squirrel-Cage Induction Machines', PhD thesis, Aalto University School of Science and Technology, Espoo, Finland. http://lib.tkk.fi/Diss/2010/isbn9789526032863/.

Liu, R., Mi, C. C. and Gao, D. W. (2008), 'Modeling of eddy-current loss of electrical machines and transformers operated by pulsewidth-modulated inverters', *IEEE Trans. Magn.* **44**(8), 2021–2028.

Lubin, T., Mezani, S. and Rezzoug, A. (2010), 'Analytic calculation of eddy currents in the slots of electrical machines: Application to cage rotor induction motors', *IEEE Trans. Magn.* **47**(11), 4650–4659.

Meeker, D. (2009), 'Finite element method magnetics', *Users Manual*. **Version 4.2**.

Mesrobian, A. and Holdrege, J. (1990), Random wound versus form wound on low voltage synchronous generators, *in* 'Petroleum and Chemical Industry Technical Conference. PCIC 1990'.

Pham, M.-T., Ren, Z., Li, W. and Koh, C.-S. (2011), 'Optimal design of a thomson-coil actuator utilizing a mixed-integer-discrete-continuous variables global optimization algorithm', *IEEE Trans. Magn.* **47**(10), 4163–4166.

Pyrhönen, J., Jokinen, T. and Hrabovcova, V. (2009), *Design of Rotating Electrical Machines*, John Wiley and Sons Ltd, The Atrium, Southern Gate, Chichester, West Sussex, PO19 8SQ, United Kingdom.

Repo, A.-K. (2008), 'Numerical Impulse Response Tests to Identify Dynamic Induction-Machine Models', PhD thesis, Helsinki University of Technology, Finland. http://lib.tkk.fi/Diss/2008/isbn9789512292752/.

Repo, A.-K., Niemenmaa, A. and Arkkio, A. (2006), Estimating circuit models for a deep-bar induction motor using time harmonic finite element analysis, *in* 'Int. Conf. Electrical Mach., Crete, Greece'.

Roy, R. K. (2001), *Design of Experiments Using The Taguchi Approach*, John Wiley and Sons, Inc., Canada.

Saari, J. (1998), 'Thermal Analysis of high-speed induction motors', PhD thesis, Helsinki University of Technology, Espoo, Finland. http://lib.tkk.fi/Diss/199X/isbn9512255766/.

Shi, T., Qiao, Z., Xia, C., Li, H. and SongZhang, Z. (2012), 'Modeling, analyzing, and parameter design of the magnetic field of a segmented halbach cylinder', *IEEE Trans. Magn.* **48**(5), 1890–1898.

Sonnaillon, M., Bisheimer, G., De Angelo, C. and Garcia, G. (2007), 'Automatic induction machine parameters measurement using standstill frequency-domain tests', *IET Electr. Power Appl.* **1**(5), 833–838.

Stermecki, A., Biro, O., Bakhsh, I., Rainer, S., Ofner, G. and Ingruber, R. (2012), '3-D finite element analysis of additional eddy current losses in induction motors', *IEEE Trans. Magn.* **48**(2), 959–962.

Stumberger, G., Dolinar, D. and Grcar, B. (1998), 'Calculation of the linear induction motor model parameters using finite elements', *IEEE Trans. Magn.* **34**(5), 3640–3643.

Stumberger, G., Stumberger, B. and Dolinar, D. (2004), 'Identification of linear synchronous reluctance motor parameters', *IEEE Trans. Ind. Appl.* **40**(5), 1317–1324.

Stumberger, G., Stumberger, B., Dolinar, D. and Hamler, A. (2001), 'Cross magnetization effect on inductances of linear synchronous reluctance motor under load conditions', *IEEE Trans. Magn.* **37**(5), 3658–3662.

Sudhoff, S., Aliprantis, D., Kuhn, B. and Chapman, P. (2002), 'An induction machine model for predicting inverter-machine interaction', *IEEE Trans. Energy Convers.* **17**(2), 203–210.

Sudhoff, S., Aliprantis, D., Kuhn, B. and Chapman, P. (2003), 'Experimental characterization procedure for use with an advanced induction machine model', *IEEE Trans. Energy Convers.* **18**(1), 48–56.

Toman, M., Stumberger, G. and Dolinar, D. (2008), 'Parameter identification of the Jiles-Atherton hysteresis model using differential evolution', *IEEE Trans. Magn.* **44**(6), 1098–1101.

Uler, G., Mohammed, O. and Koh, C.-S. (1995), 'Design optimization of electrical machines using genetic algorithms', *IEEE Trans. Magn.* **31**(3), 2008–2011.

Wrobel, R., Mlot, A. and Mellor, P. (2012), 'Contribution of end-winding proximity losses to temperature variation in electromagnetic devices', *IEEE Trans. Ind. Electron.* **59**(2), 848–857.

Wu, L., Zhu, Z., Staton, D., Popescu, M. and Hawkins, D. (2012), 'Analytical model of eddy current loss in windings of permanent magnet machines accounting for load', *IEEE Trans. Magn* **48**(7), 2138–2151.

Yamazaki, K. (2002), 'An efficient procedure to calculate equivalent circuit parameter of induction motor using 3-D nonlinear time-stepping finite-element method', *IEEE Trans. Magn.* **31**(2), 1281–1284.

Yamazaki, K., Fukushima, Y. and Sato, M. (2009), 'Loss analysis of permanent-magnet motors with concentrated windings-variation of magnet eddy-current loss due to stator and rotor shapes', *IEEE Trans. Ind. Appl.* **45**(4), 1334–1342.

Yamazaki, K.; Kanou, Y. (2010), 'Shape optimization of rotating machines using time-stepping adaptive finite element method', *IEEE Trans. Magn.* **46**(8), 3113–3116.

Yamazaki, K., Kuramochi, S., Fukushima, N., Yamada, S. and Tada, S. (2012), 'Characteristics analysis of large high speed induction motors using 3-D finite element method', *IEEE Trans. Magn.* **48**(2), 995–998.

Yamazaki, K. and Watari, S. (2005), 'Loss analysis of permanent-magnet motor considering carrier harmonics of pwm inverter using combination of 2-D and 3-D finite-element method', *IEEE Trans. Magn.* **41**(5), 1980–1983.

Zhang, D., Park, C.-S. and Koh, C.-S. (2012), 'A new optimal design method of rotor slot of three-phase squirrel cage induction motor for nema class d speed-torque characteristic using multi-objective optimization algorithm', *IEEE Trans. Magn.* **48**(2), 879–882.

Zhao, N., Zhu, Z. and Liu, W. (2011), 'Rotor eddy current loss calculation and thermal analysis of permanent magnet motor and generator', *IEEE Trans. Magn.* **47**(10), 4199–4202.

Publication Errata

Publication III

The equation (15) to calculate rotor resistive loss is corrected as follows

$P_{\mathrm{rt}} = \frac{3}{2}\left(R_{\mathrm{r}1} I_{\mathrm{r}1}^2 + R_{\mathrm{r}2} I_{\mathrm{r}2}^2 + R_{\mathrm{r}3} I_{\mathrm{r}3}^2 + R_{\mathrm{c}2} I_{\mathrm{r}12}^2 + R_{\mathrm{c}1} I_{\mathrm{r}}^2\right)$

where

$\underline{i}_{\mathrm{r}} = \underline{i}_{\mathrm{r}1} + \underline{i}_{\mathrm{r}2} + \underline{i}_{\mathrm{r}3}$

$\underline{i}_{\mathrm{r}12} = \underline{i}_{\mathrm{r}1} + \underline{i}_{\mathrm{r}2}$

Publication IV

The stator impedance in (12) is modified

$\underline{Z}_{\mathrm{s}}(s) = R_{\mathrm{s}} + \frac{sL_{\sigma\mathrm{s}}(R_{\mathrm{e}}+sL_{\mathrm{se}})}{sL_{\sigma\mathrm{s}}+R_{\mathrm{e}}+sL_{\mathrm{se}}}$

The equation (13) is corrected as

$\underline{Z}_{\mathrm{r}}(s) = R_{\mathrm{c}} + (s - j\omega_0) L_{\mathrm{c}} + \underline{Z}_{\mathrm{r}12}$

where

$\underline{Z}_{\mathrm{r}12} = \frac{((s-j\omega_0)L_{\mathrm{r}1})(R_{\mathrm{r}2}+(s-j\omega_0)L_{\mathrm{r}2})}{(s-j\omega_0)L_{\mathrm{r}1}+R_{\mathrm{r}2}+(s-j\omega_0)L_{\mathrm{r}2}}$

Aalto-DD 162/2012

ISBN 978-952-60-4891-8
ISBN 978-952-60-4892-5 (pdf)
ISSN-L 1799-4934
ISSN 1799-4934
ISSN 1799-4942 (pdf)

Aalto University
School of Electrical Engineering
Department of Electrical Engineering
www.aalto.fi

BUSINESS + ECONOMY

ART + DESIGN + ARCHITECTURE

SCIENCE + TECHNOLOGY

CROSSOVER

DOCTORAL DISSERTATIONS